

# CIESIN Thematic Guide to Night-time Light Remote Sensing and its Applications

Christopher N.H. Doll

December 2008

Center for International Earth Science Information Network (CIESIN)  
Columbia University  
Palisades, NY, USA



**Sponsored by the Socioeconomic Data and Applications Center (SEDAC) of the  
U.S. National Aeronautics and Space Administration,  
Goddard Space Flight Center under contracts NAS5-03117 and NNG08-HZ11C**

Copyright © 2008  
The Trustees of Columbia University in the City of New York.

Available on the web at <http://sedac.ciesin.columbia.edu/tg/>.

## 1. Title & Abstract

### Thematic Guide to Night-time Light Remote Sensing and its Applications

Christopher N.H. Doll<sup>1</sup>

#### Abstract

Night-time light imagery stands unique amongst remote sensing data sources as it offers a uniquely ‘human’ view of the Earth’s surface. The presence of lighting across the globe is almost entirely due to some form of human activity be it settlements, shipping fleets, gas flaring or fires associated with swidden agriculture. This extensively illustrated guide introduces users to the types of night-time light data available, its characteristics and limitations. It details the distinguishing features of the stable lights, radiance calibrated and time series Average DN datasets. The latter currently spans the period 1992-2003. The spatial and temporal characteristics of the datasets are presented using a range of techniques including temporal color composites. Preliminary analysis of this time series reveals considerable differences in brightness between data collected from different platforms. The second part of the guide examines how this interesting data source has been used and may be used to derive useful information about human presence and practice on Earth. Topics range from population and light pollution to economic activity, greenhouse gas emissions and using night-time lights to help with disaster management. Consideration is also given to the ecological ramifications of night-time lighting. With these elements set out, the final section explores other potential sources of night-time light data and how future systems may enhance our existing capabilities to understand the human environment through this the observation of lights at night.

<sup>1</sup> Formerly with the Center for International Earth Science Information Network (CIESIN), Columbia University, Palisades, NY, USA, and currently with the International Institute for Applied Systems Analysis (IIASA), Laxenburg, Austria. Email: doll -at- iiasa.ac.at

## Contents

1. Title & Abstract .....	3
2. Introduction .....	5
3. The DMSP-OLS sensor and its data products .....	6
3.1. Description .....	6
3.2. Types of Product.....	7
3.2.1. Stable Lights .....	8
3.2.2. Radiance-calibrated data.....	9
3.2.3. Average Digital Number.....	10
3.2.4. Comparison Among the Datasets .....	11
3.3. Strengths and Limitations of the Data Sets.....	11
3.3.1 Spatial Characteristics .....	12
3.3.2. Temporal Characteristics .....	14
3.3.3. Considerations .....	17
4. Applications of DMSP-OLS.....	18
4.1. Urban Extents .....	18
4.2. Population.....	19
4.3. Economic Activity.....	22
4.4. Greenhouse Gas Emissions .....	24
4.5. Light Pollution.....	26
4.6. Disaster Management .....	28
5. Other sources of current and future night-time light data .....	31
5.1. Astronaut photography .....	31
5.2. Dedicated airborne missions.....	32
5.3. Nightsat Mission.....	34
Glossary of Terms .....	36
Figure Credits .....	37
References .....	38

## Acknowledgements

The author gratefully acknowledges the peer-review comments by Dr. Paul Sutton of the University of Denver and Dr. Christopher Small of the Lamont-Doherty Earth Observatory at Columbia University. Dr. Christopher Elvidge of the National Oceanic and Atmospheric Administration (NOAA) National Geophysical Data Center also provided useful advice during various stages of the preparation of this Guide. Finally, he wishes to thank Alex de Sherbinin at CIESIN, The Earth Institute of Columbia University, for contributions and editorial suggestions, as well as for shepherding the guide through to publication. Any deficiencies of the final product are the responsibility of the author.

*Suggested citation:* Doll, C.N.H. 2008. *CIESIN Thematic Guide to Night-time Light Remote Sensing and its Applications*, Palisades, NY: Center for International Earth Science Information Network of Columbia University. Available on-line at <http://sedac.ciesin.columbia.edu/tg/>.

Work for this thematic guide was supported by the U.S. National Aeronautics and Space Administration, Goddard Space Flight Center under contract NAS5-03117 (for the Socioeconomic Data and Applications Center). The views expressed in this guide are not necessarily those of CIESIN, SEDAC, Columbia University, or NASA.

## 2. Introduction

*Cities, like cats, will reveal themselves at night.*  
Rupert Brooke, Letters from America

The presence of light across the Earth's surface provides some of the most visually stunning and thought provoking scenes from space. The discovery that lights could be observed at night from a sensor that was initially conceived to observe clouds at night is one of the most fortuitous unforeseen benefits to have come from remote sensing technology. Whilst we are often in awe of scenes of outstanding natural beauty, what is stunning about night-time light imagery is that its presence is almost entirely human induced and gazing upon the Earth at night leaves us in little doubt of our capacity to modify our planet on a global scale at great speed. In the 2 centuries since Humphrey Davy first demonstrated a light bulb to the Royal Society in 1806, there isn't a single country in the world where light cannot be detected. However there are more lights in some places than others. The relative brightness and spatial extent of lights can offer clues and insights into a whole range of human activities and enable scientists to gain a uniquely human perspective on the world.

This guide covers the description and applications of the Defense Meteorological Satellite Program-Optical Line Scanner (DMSP-OLS) sensor. It takes a step by step look at the sensor and how it acquires the images and describes the data products that are available. Looking beyond the presence of lights, this guide will show the truly interdisciplinary nature of applications that can be considered with the use of night-time lights and will leave the reader in no doubt of how so many hitherto unconnected elements of human activity can be explored, described, modeled or mapped with night-time light data. Whilst the bulk of the guide deals with the imagery from the DMSP-OLS data set, the final section, presents other sources of night-time light data, at higher spatial resolutions offering insights into the future products and applications of light data.

Night-time lights provide a versatile and user friendly data source for the social scientist, whether it is used simply to define an urban area or used more intensively to model population, economic activity or some other socio-economic parameter. The studies and applications discussed here represent the main body of work done with these data.

With an understanding of what the lights show (and do not show), the reader will understand their value for research questions concerning the urban environment, and how their utility is greatly increased by combining them with other data sets that help to overcome the data set's limitations.

### 3. The DMSP-OLS sensor and its data products

This section describes the key elements and attributes DMSP-OLS sensor. The description reviews its history and how it acquires imagery at night. It then goes on to discuss the main the types of data products which are available for analysis.

#### 3.1. Description

The Defense Meteorological Satellite Program, (DMSP) is the meteorological program of the US Department of Defense, which originated in the mid-1960s with the objective of collecting worldwide cloud cover on a daily basis (Kramer, 1994). The system was officially acknowledged and declassified in 1972 and made available to the civilian/scientific community (NASA, 1997). The DMSP programme has been repeatedly upgraded over time since declassification (SMC, 1997); the latest series (Block-5D) incorporates the Operational Linescan System (OLS). The DMSP satellite (Figure 1) flies in a sun-synchronous low earth orbit (833km mean altitude) and makes a night-time pass typically between 20.30 and 21.30 each night (Elvidge *et al.*, 2001a). Orbiting the Earth 14 times a day means that global coverage can be obtained every 24 hours. The OLS sensor has two broadband sensors, one in the visible/near-infrared (VNIR, 0.4 – 1.1 $\mu\text{m}$ ) and thermal infrared (10.5 – 12.6 $\mu\text{m}$ ) wavebands. (An explanation of the electromagnetic spectrum can be found in section 3.3 of the CIESIN Thematic Guide to Social Science Applications of Remote Sensing.) The OLS is an oscillating scan radiometer with a broad field of view (~3,000km swath) and captures images at a nominal resolution of 0.56km, which is smoothed on-board into 5x5 pixel blocks to 2.8km. This is done to reduce the amount of memory required on board the satellite.



**Figure 1. Artists impression DMSP block 5 series satellite.**

Cross-track scanning sensors use a wide range of scan angles to acquire images and therefore suffer from two geometric problems. One is known as the bi-directional reflectance distribution function (BRDF), which describes the variation in reflectance of a surface for a given view and illumination angle. The other is a geometric distortion in pixel size as the scan moves increasingly off nadir (away from vertical). Low-level light amplification in the visible channel is facilitated

through the use of a photomultiplier tube (PMT) so clouds illuminated by moonlight at night can be observed. The **gain** applied to the signal varies every 0.4 milliseconds based on the predicted illumination of the scene from solar elevation and lunar phase and elevation. In addition to this, a BRDF algorithm further modifies the gain where the illumination angle approaches the observation angle to take advantage of the enhanced 'hot spot' of **specular reflection**. The OLS employs a sinusoidal scan motion, which maintains a nearly constant pixel to pixel ground sampling distance of 0.56km at all scan angles in fine resolution data mode. It has been specially designed to exploit the rotation of the scanning motion in order to reduce the expansion of the viewed area at high scan angles.

These features not only permit the detection of visible band light sources down to  $10^{-9}$  Watts/cm<sup>2</sup>/sr but also produce visually consistent imagery of clouds at all scan angles. The sensitivity of the OLS sensor is some four orders of magnitude greater than other sensors such as NOAA-AVHRR or Landsat Thematic Mapper (Elvidge *et al.*, 1997a), a feature that makes it unique amongst environmental remote sensing satellites. Although this was done with the initial aim of producing night-time cloud imagery on which to base short term cloud cover forecasts, a fortuitous unforeseen benefit was also discovered: city lights, gas flaring, shipping fleets and biomass burning can also be detected in the absence of cloud cover (Croft, 1978).

Digital OLS data was not made available by the US Department of Defense and subsequently was not archived by the National Oceanic and Atmospheric Administration's National Geophysical Data Center (NOAA-NGDC) from the time of declassification until 1992. Prior to this, scientific access to the data could only be obtained from a film archive. Despite this limitation, its potential as an indicator of human activity was noted by Croft (1978), Welch (1981), who analysed the correlation of lit area and energy consumption for selected American cities, and Sullivan (1989), who created the first global cloud free composite at a spatial resolution of 10 arc-minutes from data collected between 1974-84. A digital archive of night-time light imagery has been established since 1992 from which a number of global data sets has been produced. The dissemination of these data allowed for more detailed and quantitative analysis than had previously been possible. A range of these are presented in section 4.

### 3.2. Types of Product

Since digital archiving began, a number of products have been released. There were initially two types of night-light data available: the frequency composite and a maximum pixel value for the cloud free orbits. The latter has since been withdrawn. At the time of writing, there are currently three processed versions of night-time light data sets products which are released by NOAA-NDGC. Individual orbits can always be downloaded for individual processing should data over a specific area and time be needed. Whilst they are all based on the same fundamental imagery, there are important processing steps to be aware of when deciding which product to use. This choice will be dictated by the time (year), the information content of the imagery, and the whether temporal updates will be needed.

There are three different types of imagery associated with the DMSP-OLS data set.

- Frequency detection (Stable lights)
- Radiance calibrated
- Average Digital Number

These are described in the following sections and briefly contrasted in section 3.3.

### 3.2.1. Stable Lights

The digital archiving of DMSP-OLS data provided a catalyst for renewed interest in using this data source to advance the tentative observations initially made from OLS film data. The work of Christopher Elvidge and his team at NOAA-NGDC in Boulder, Colorado, in creating a ‘stable lights’ product represents the single greatest advance in the processing of OLS night-time light data. This product used six months’ worth of imagery acquired between October 1994 and March 1995 during periods of low lunar illumination. Whilst lunar illumination was crucial to imaging clouds at night, it is a hindrance to observing light sources from the ground due to the reduced contrast of light sources from the ground. Other hindrances include glare from scattered sunlight and bad scan lines. Filtering out bad scan lines (defined as 10 consecutive lights with no lights above or below) also removes lit pixels caused by lightning (Elvidge, 2005). Over the six-month period a temporal composite was built up of cloud free images of the earth at night. Compositing not only allowed clouds to be excluded, but also facilitated the analysis of ‘stable lights’. The presence of stable lights is important in distinguishing different light sources (e.g. city lights, shipping fleets or forest fires). However, the variation in brightness between orbits means that it is not possible to establish a single digital number (DN – or at sensor radiance) threshold for identifying VNIR emission sources (Elvidge et al. 1997a).

To overcome this, an algorithm was developed to automatically detect light using a nested configuration of 200x200 and 50x50 pixel blocks. The light-picking algorithm applies a threshold to the central 50x50 pixel block based on the histogram of the surrounding 200x200 pixel block. Background pixels are identified by working down the frequency distribution from the brightest pixel to identify the first DN value where five consecutive DN values have greater than 0.4 % (10 pixels) of the total pixel counts. The threshold is established by calculating the mean plus four standard deviations of those background pixels. This threshold is then applied to the inner pixel block to identify pixels that are determined as being lit. There is a 60% overlap in area of the 200x200 pixel blocks used to generate the background pixels between adjacent 50x50 pixel blocks which results in a smooth transition between threshold levels in each 200x200 pixel block (Elvidge *et al.*, 2003).

Using this detection algorithm, the pixel value is assigned according to the percentage of times light was detected during cloud-free overpasses. Analysing the temporal frequency and stability of lights can help to distinguish their most likely source. City lights can be identified because they are temporally stable. However, forest fires can also be identified due to their location and lack of temporal stability over the compositing period. Through this process, the global night-time light composite can be filtered into a variety of different products:

- lights from human settlements and industrial facilities (city lights)
- fires
- gas flaring
- shipping fleets

A geolocation algorithm was used to map the data onto the 1km grid developed for the NASA-USGS Global 1km AVHRR project (Eidenshink and Faundeen, 1994). City-lights accounted for most of the light emissions seen from space at night from this product. However, there were also contributions from other sources such as shipping fleets (common in the Sea of Japan and off Argentina), gas flaring and biomass burning in sub-Saharan Africa, the Amazon and SE Asia. These tended to be highly regional in nature. To download the data see “Night-time lights of the world, 1994-1995” in the References.

One issue with this data set is that certain areas of the globe receive more cloud-free views than others. This creates problems for the fire product, which often occurs in cloud-covered tropical regions. It should be noted that NOAA-NDGC do not feel 6 months worth of data was sufficient to fully discriminate between stable lights and fire. This is currently being investigated using dedicated fire products from other satellites such as MODIS, part of NASA's Earth Observation System.

One of the biggest problems encountered with this first version of night-time lights was low-light level **pixel saturation**. A new product was planned, which attempted to increase the detectable radiance range by varying the gain on the sensor thereby reducing the saturated area over city centres.

### 3.2.2. Radiance-calibrated data

The problems of relatively low-level pixel saturation from the 6-bit sensor over bright urban areas led to the experimentation and ultimate production of a new low-gain data set. Elvidge *et al.* (1999) described a method for detecting a greater range of settlements than in the 1994-95 product by varying the gain of the sensor. Low gain experiments were conducted in March 1996 to identify the gain settings that produce the best results. Such is the effect of the gain that sensor saturation can occur over a range of more than two orders of magnitude, likewise for the minimum detectable radiance value. Based on these experiments, two gain settings at 24dB and 50dB were selected and were alternately applied to each 24-hour set of acquisitions taken in January and February 1997. The thresholding technique used to create the stable lights data set was found to perform poorly at identifying diffuse lighting, which is often dim and spatially scattered across the landscape. Such features were manually identified via the development of a software tool, which also provided a means of quality control for the product.

High and low gain cloud-free composites were averaged. The radiance-calibrated average DN from each image was weighted by the total number of detections. The final data set contained calibrated radiances between  $1.54 \times 10^{-9}$  and  $3.17 \times 10^{-7}$  Watts/cm<sup>2</sup>/sr and was produced in byte (0-255) format at 30 arc-seconds (1km). The conversion from DN to radiance is given in the formula:

$$\text{Radiance} = (\text{Digital Number})^{3/2} \text{ Watts/cm}^2/\text{sr}$$

The range was made deliberately ample on either side to allow for any future variations in gain. Since the DN variation is a physically meaningful quantity as opposed to a 'lit-frequency' observation, this makes it a flexible data set for use in a variety of modelling schemes subject to finding appropriate relationships between radiance and the parameters of interest. Low gain data for generation of an improved global radiance calibrated nighttime lights product has been acquired at the turn of the millennium but has, as yet not been processed into a global data product so only the 1996-97 data set is available for download (see "Radiance Calibrated Lights, 1996-1997" in the References). Radiance calibrated data for 2001 has been produced for the conterminous United States as part of a study to map impervious surfaces for analysing the impact of development sprawl. This is also available for download (see "Radiance Calibrated Lights, 2001" in the References).

### 3.2.3. Average Digital Number

The latest and now most extensive release of night-time light data comes in the form of average Digital Number (DN) values. This version was originally presented as their change product, and initially offered two global coverages, 1992-93 and 2000, and a change product.

The data was processed to use the high quality visible band data. Pixels were screened to remove those with lunar illumination, glare, bad scanlines and lightning and other marginal data (Elvidge et al., 2005). As with the stable lights, cloud screening was done using the thermal channel. Rather than using the onboard BRDF correction algorithm, only the centre halves of orbital scans were used discarding the outer quarters in a manner consistent with the radiance calibrated imagery. This consistent use of imagery from similar parts of the scan avoids the large differences in brightness possible from extreme view angles. Images were manually inspected for blooming conditions (see section 3.3.1 for an explanation of this phenomenon).

This has recently been extended to a full archive of data from every sensor for every year. This facilitates the analysis of changing lighting patterns in the following ways:

- The appearance of new light sources
- The disappearance of light sources
- The expansion and contraction of light sources
- Positive and negative changes in the brightness of lights.

There are 14 years worth of data available at near global coverage, full longitudinal (East/West) coverage (-180° to 180°) and partial latitudinal (North/South) coverage from -65° to 65° North. This area excludes the northern parts of Scandinavia, Canada and Alaska, where there are few lights but does capture the main cities in these countries. Four satellites (F-series) were used to collect the 14 years of data and there are six sets of co-temporal data to be compared between three pairs of satellite. These are listed in the table below.

Satellite Series	Years	Co-temporal years with next series
F10	1992-1994	1994
F12	1994-1999	1997,1998,1999
F14	1997-2002	2001, 2002
F15	2001-2003	

This is a relatively new data set, expanding on the 1992-93 and 2000 change pair. As such, there is little information about how the data varies from year to year, however, some issues and caveats are described in the section 3.3.2 on temporal considerations. To download the data see Version 2 DMSP-OLS Nighttime Lights Time Series in the References.

Another version of night-time lights yet to be released to the public takes the current global annual composites and divides the DN values by the frequency of observation of the lights over the course of that year to derive what is known as the lights index. The conceptual basis being that the brightness of lights can be further classified by taking into account how often that light is observed to be lit in the cloud-free observations. This version of the lights (version 3) was used in some recent research papers and researchers should be careful to note which version was used.

In addition to the freely available standard processed night-time lights products listed here, individual passes for a specific date may be purchased by orbit (from the equator making a full orbit back to the equator), suborbit (a subsection thereof), and geo-located data. For access to these data see DMSP Data Services and Pricing in the References.

**3.2.4. Comparison Among the Datasets**

A visual comparison is presented below in Figure 2 to gain an appreciation of the differences between the three data sets described above. It is apparent the initial stable lights product has far less variation than the other two and the imagery saturates very rapidly at the maximum 100 percent frequency detection value. The stable lights product is based on the 6-bit (0-63) quantization shown with the average DN values. This product also has a large number of pixels taking the highest range of values. The distribution of values is spread more evenly in the radiance-calibrated version with, with the majority of pixels in the low range and only very few at the brightest radiance values indicating sensor saturation (even with the gain turned down).

In terms of the spatial extent of the detected lit areas, the average DN data set shows the most lit area, followed by the radiance calibrated data set. This is because they have not been filtered or thresholded to the same extent as the stable lights data set, which deals exclusively with city lights. The reason why the average DN data set depicts the largest lit area is addressed in section 3.3.1

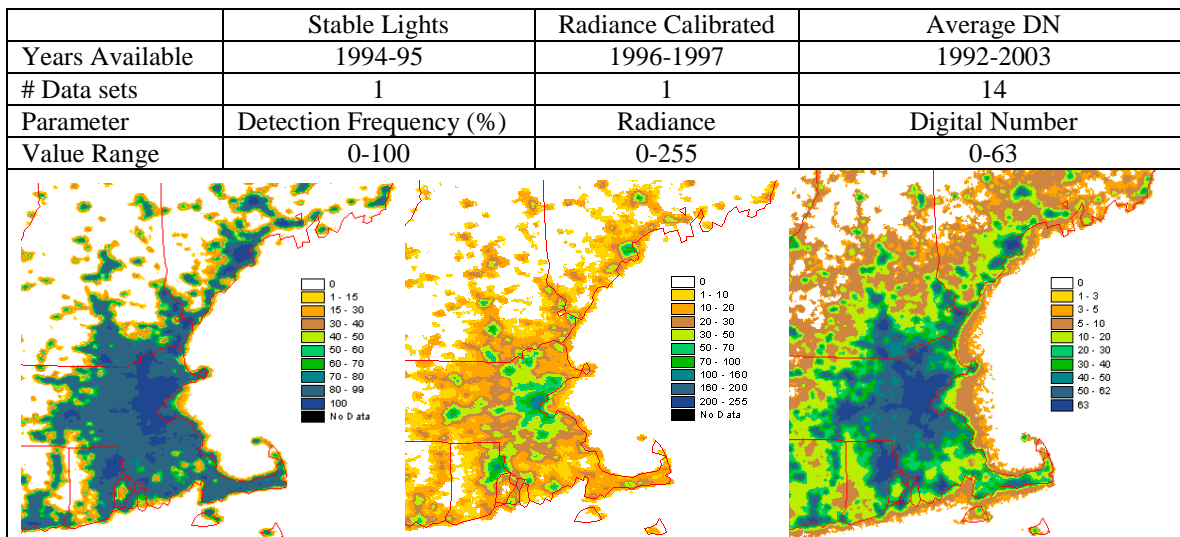


**Figure 2. Comparison of the three different data sets over a portion of New England (from left to right: Stable Lights, Radiance Calibrated, and Average DN)**

**3.3. Strengths and Limitations of the Data Sets**

There are both spatial and temporal properties of the DMSP-OLS data set which affect the efficacy of the data set for its range of applications. Essentially these relate to changes in the spatial extent of lit areas and variations in the brightness of a pixel over time. Depending on the

nature of the application at hand, the relative importance of spatial extent versus information content (DN) will vary. Understanding how lights behave in space and time will lead to the sound scientific use of the data set and minimize misinterpretation of the results.

### 3.3.1 Spatial Characteristics

The principal spatial consideration to bear in mind when working with night-time light imagery is the extent to which the spatial area depicted on images matches the true extent of lit area on the ground. Imagery from the DMSP-OLS satellite has a tendency to overestimate this parameter, an effect generally referred to as “blooming” (and more recently “overglow”) in the literature. Small *et al.* (2005) cite three main reasons for this phenomenon, which are discussed briefly.

- **Coarse spatial resolution**

Although the DMSP-OLS sensor has a nominal resolution of 1km, this has been resampled from the 2.7km native resolution of the sensor. An inherent feature of satellite imagery is that it will generalize ground based features to a single DN or radiance value. In the case of night time light imagery, this manifests itself as pixels appearing lit, when the light source is not being emitted over the entire pixel area. Examples of higher resolution night-time light imagery and how it compares to the DMSP-OLS can be found in section 5.1 and 5.2. A general discussion of scale and resolution and the problem of “mixed pixels” in remote sensing can be found in sections 3.3 and 3.5 of the CIESIN Thematic Guide to Social Science Applications of Remote Sensing.

- **Large Overlap between pixels**

A feature of the data acquisition process is that there is a large overlap (some 60%) between pixels. This means that light observed in one location has the chance to be recorded in more than one pixel. This can contribute to a larger lit-area being detected than is actually the case.

- **Errors in the geolocation**

Errors are inherent in the projection process. Data is recorded in arrays, the spatial position of these data values are calculated from the navigation data onboard the satellite. These values are then projected onto a 1km grid. The grid itself is an approximation of the Earth’s surface corrected for the topographic variation. Each transformation introduces errors into the process.

To this a fourth factor, the atmospheric water vapour content can be added. Lights can appear dimmer and more spatially diffuse where thin clouds are present, which is consistent with similar effects of image quality reduction for other optical (or “passive”) sensors.

The combined effect of these factors ultimately results in a general overestimation of area, which can be deceiving due to the visually stunning nature of the data set. Figure 3 illustrates the blooming effect, and also shows different sources of light that can be observed from the DMSP-OLS sensor. It is apparent that cities appear lit, but so too do traffic on unlit sections of highway and areas that are unlit but which are affected by overglow.

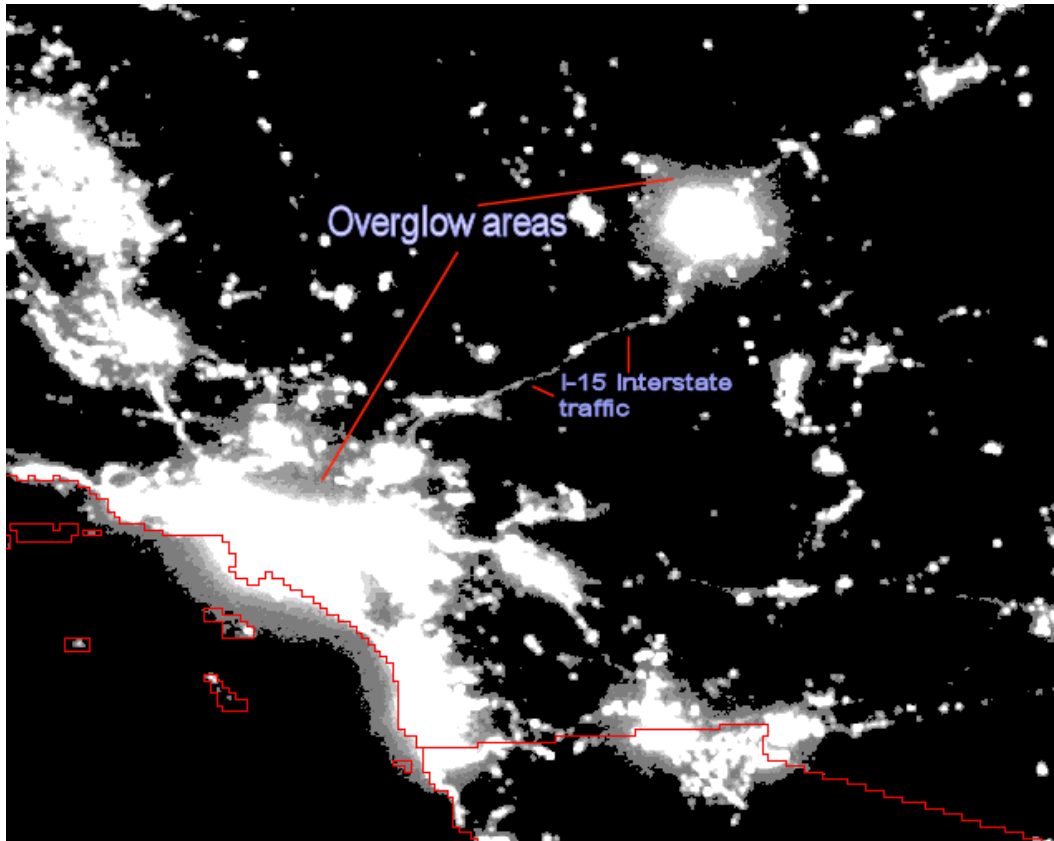


**Figure 3.** A detail from the DMSP-OLS average DN data set from 2002. Night-time lights contrast enhanced to show the overflow surrounding bright urban centers. Note how light is detected more than 50 kilometers offshore from Los Angeles. Overflow digital number (DN) values exceed DN values for lighting from Interstate 15 highway traffic and many small towns.

To correct this effect, thresholding (excluding values below a certain value) has been used to reduce the area of the lights. Previous studies have identified thresholds ranging from 80-97% for different cities in the US (Imhoff *et al.*, 1997). However, it soon becomes apparent that there is no single threshold that can be applied which would match the urban delimitation for all cities. In particular, thresholding large urban areas tends to result in the attenuation of lights associated with smaller settlements. The implication of this finding is that a range of thresholds needs to be applied depending on the size of the settlement involved. Research conducted by Small *et al.* (2005) examined the stable lights 1994-95 and change pair 1992-2/2000 DMSP-OLS data sets in conjunction with Landsat imagery and found that lighted area estimates are larger than the maximum estimates of built area from Landsat for almost every city in the lights data set. Respective thresholds of 10 and 14% for the 1994-95 and change pair data sets were found to optimize the trade off between reducing lit area to match city size and attenuating lights of smaller settlements. Their comparison of lit area with overflow extent revealed a linear proportionality and suggests that a scale dependent overflow correction model could be developed, in order to 'shrink' the lights down to more closely match their built-up area. This proportional correction was tentatively put at 1.25 of lit to built diameter, subject to further study.

### 3.3.2. Temporal Characteristics

Until recently, there has been little in the way of temporal analysis of the DMSP-OLS night-time light products owing to the lack of a temporally consistent data set with which to assess changes. The release of annual data from 1992-2003 described in section 3.2.3, paves the way for a rigorous undertaking of this analysis. There are at present no published articles detailing these differences. Some work has been done with the 1992/3 and 2000 change pair data set. Low-level pixel saturation in both the 1992-93 and 2000 data sets prevent city centre analysis, but it does allow investigation of the spatial expansion of lights in peri-urban areas. Furthermore, the 1992, 1998 and 2003 versions of this average DN data set (released prior to the full 14 years data) have been used to investigate temporal changes. This method involves constructing tri-band red, green, blue false color composites with a different year for each channel. The convention has been to put the 1992 year through the red channel, 1998 in the blue, and 2003 in green. Superimposition of these channels can reveal whether lighting has been lost (red hues), gained (green hues) or emerged then disappeared (blue hues). This is most striking in places which have undergone massive economic/political change such as the countries of Eastern Europe following the fall of communism and the transition to free market economies. In Figure 4, we see that the former Soviet republics of Ukraine and Moldova are dominated by red hues indicating lights were most prevalent in 1992 and then declined in 1998 and 2003. This is sharply contrasted by Poland and Romania to the west whose greener and bluer hues indicate spatial expansion and brightening of lights.

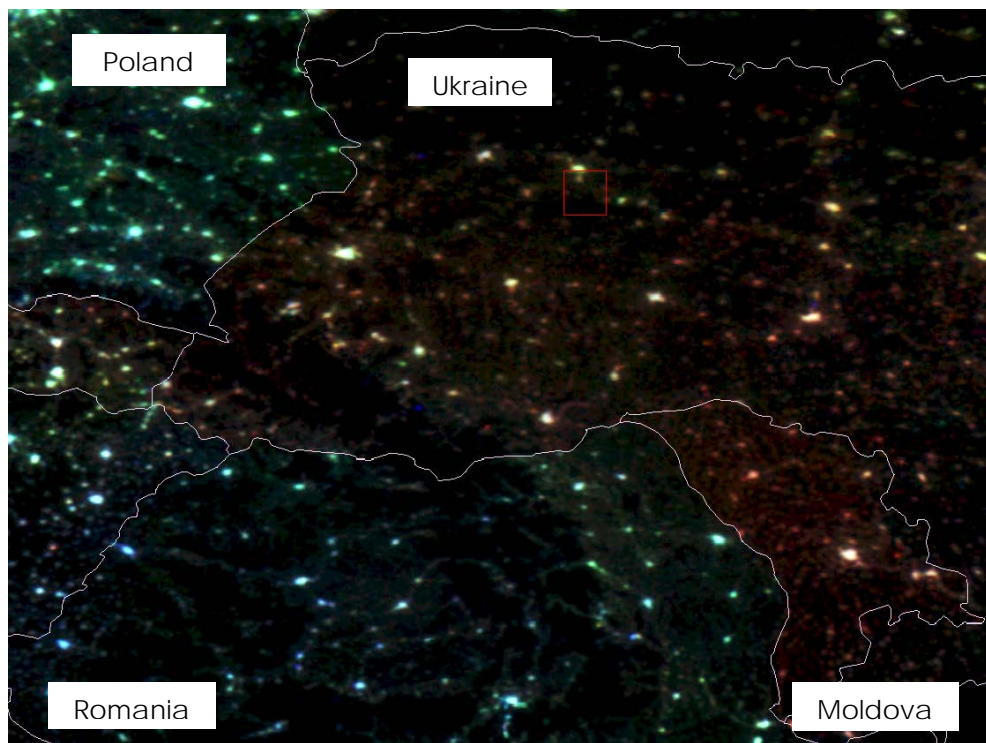


**Figure 4. Temporal colour composite over Eastern Europe. Red: 1992, Green: 1998, Blue: 2003.**

The problem with the 3 colour composites over long time periods is that they come from sensors on board different satellites and there is no internal or cross calibration between them. For

practical purposes this means that we cannot say with any certainty whether changes in the brightness of lights are due to changing ground conditions or to changes in the sensor over time.

The latest night-time light product (1992-2003) reports the average digital number observed over the course of the entire year (2003). However, these are not radiometrically calibrated. This means that a DN value from a certain satellite year may not have the same brightness as the same DN from another year. More over, data values from one satellite may not be compatible with those from another. Preliminary research undertaken by the author suggests that there are considerable differences between the sensors on the F14 satellite (1994-1999 - which provides the green channel) for the color composite shown in Figure 4. In this situation, great care needs to be taken when interpreting the difference in brightness from sensors flying on different satellite series. The fact that there are duplicate sensor data for many years will help researchers develop some form of calibration to help interpret brightness changes over time.

*Comparing brightness*

Looking at the **total** DN of the scene, it is apparent that the F14 1997-2002 data series is consistently dimmer than the other three satellite series. Since the F14 series is co-temporal with both the F12 at its early range (1997-1999) and F15 at its late range (2001-2002), this causes a significant difference in observed brightness for the same year. There is also a similar, though less pronounced difference between the F10 and F12 value for 1994. The exception is for the year 2003, where despite maintaining a high lit area, the brightness detected by the F15 is substantially lower compared with the years from the same sensor and even compared to previous years from other sensors.

Here **total** DN is compared to GDP for India to illustrate how different years have different brightness levels. Currently, it is not known why the F14 series is consistently dimmer than other sensors in the series, or why the **total** DN for 2003 drops by 35% from the previous year. This certainly has implications for generating three band colour composites where inferences are made about development from the shades of red, blue and green present in the image.

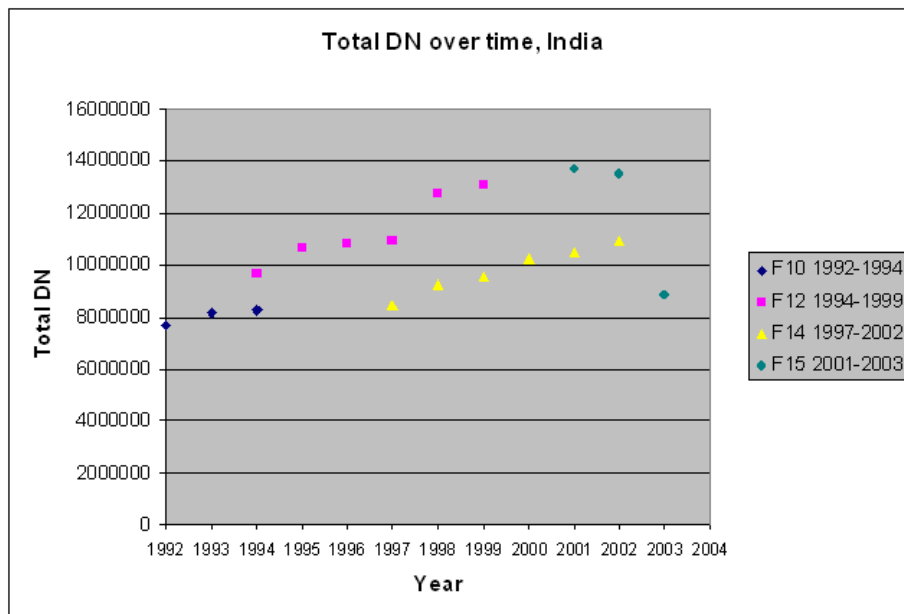


**Figure 5. Total DN for India 1992-2003 using overlapping years from 4 different DMSP-OLS sensors.**

In Figure 6, analysing the DN sum of two sensors, F12 and F14, for the same time period in 1997 (indicated with the line in Figure 5), we see that the difference in **total** DN is persistent throughout the DN range (i.e. increasing the threshold from where the **total** DN is calculated). **Total** DN values only converge at the highest levels of brightness. Attempts at cross calibrating the lights are underway. At the time of writing preliminary attempts to calibrate this series have been made to correct for these differences. Elvidge *et al.* (2007) systematically quantifies this for the years 1995-2004 with the later version 3 data set (not the version 2 currently available).

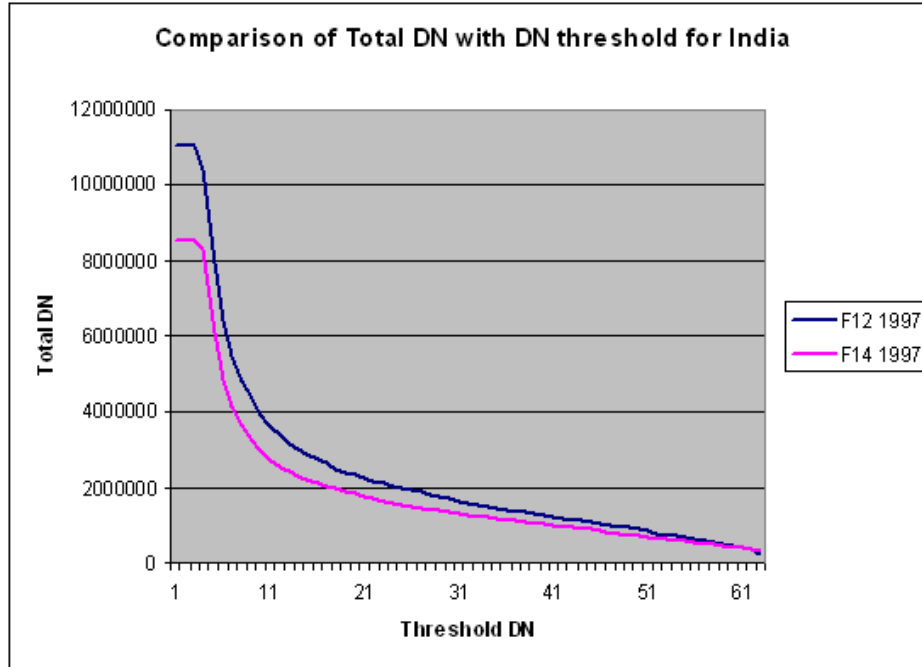


**Figure 6. Comparison of total DN over India as the sum is taken at increasingly higher thresholds. This compares F12 and F14 satellites over India in 1997.**

Although questions remain over the relative brightness of the satellite between years and series, the lit-area detected by the lights should be a more consistent parameter that can be used across platforms. Over time, certain spatial developments are clearly visible such as the lighting of the India-Pakistan border over time (Figure 7).

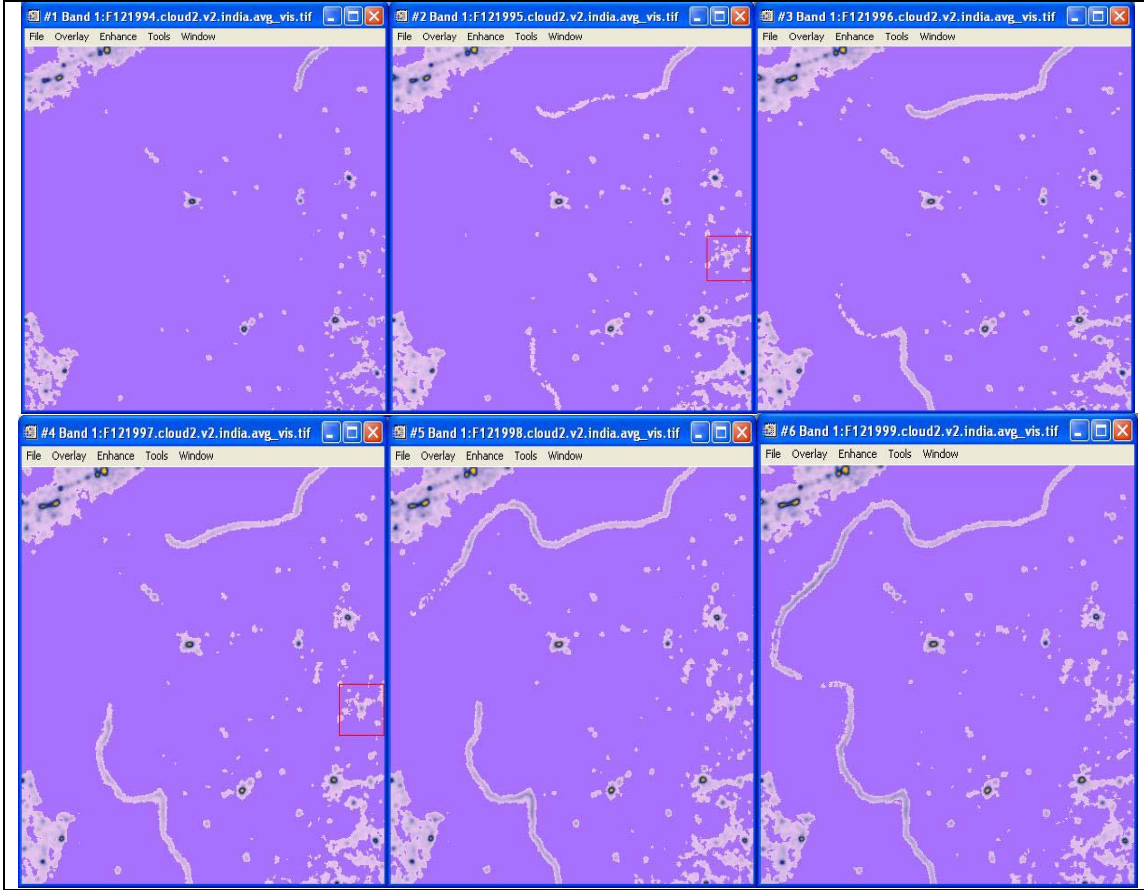


**Figure 7. Time series of showing the illumination of the Pakistani-Indian border in Rajasthan from the F12 satellite from 1994 (top left) to 1999 (bottom right).**

**3.3.3. Considerations**

Given the range of variations that can occur with the night-time lights data set, any application will need to take into account the limitations of using this data source. For applications where light will be used solely as a delimiter of urban extent, then considerations of blooming (overflow) are most pertinent. Of the two phenomena, overflow is currently the best understood and strategies exist in the literature (Small *et al.*, 2005) to account for its effects.

The recent release of temporal time series of night-time light data will allow for the study of changes in brightness over time. Currently there are no published reports which systematically analyse the changes in brightness. However early evidence suggests that the F14 series (1997-2002) has lower brightness levels compared to the others and that the data from the F15 2003 sensor also seems anomalously dim. It is recommended that these data should not be used directly in year-on-year applications but rather should be individually calibrated to the parameter in question. As yet it is not possible to say whether the sensitivity in change in DN is due more to changes in ground lighting conditions or to differences between and within sensors.

## 4. Applications of DMSP-OLS

A range of social science applications of remote sensing data is covered in the CIESIN Thematic Guide to Social Science Applications of Remote Sensing (de Sherbinin *et al.* 2002). It is not the aim of this section to repeat this here, but rather to provide a more focused description of how night-time light remote sensing data may be used to address research questions in the social sciences.

Night-time light imagery has been used for a number of other applications, the most intuitive of which is the mapping of urban areas. The ability to consistently and accurately delineate urban areas facilitates other spatial research of urban areas, including research using other remote sensing instruments. More sophisticated applications use the spatial location of the lights in conjunction with their brightness to model, estimate or map socio-economic parameters. The examples below provide a flavour of the breadth of application for the data set and discuss how the DMSP-OLS data may be used to gain insights into these issues. For a complete methodological description, the reader is advised to consult the references associated with each application.

### 4.1. Urban Extents

Global land cover maps are spatial classifications of the Earth's surface. They are traditionally focused on the major vegetated biomes and cropland areas, with urban areas being the residual. This tends to underestimate urban area. By contrast night-time light imagery explicitly maps lit areas, however the overflow characteristic described in section 3.3.1 means that the resulting maps tend to overestimate urban extent. Doll & Muller (1999a) found that unfiltered night-lights covered 20 times as much area at the continental level compared to urban delineation of the Digital Chart of the World data set (ESRI, 1997).

Imhoff *et al.* (1997) investigated how well DMSP-OLS defined urban areas in the US correspond with census data. Using an iterative thresholding technique, they established a threshold of 89% for the 1994-95 city lights data set. This threshold was identified as being the level where, on average, one could shrink the city-lights but preserve the integrity of the lit urban cluster (i.e. no internal fragmentation within the cluster). This was detected via analysis of the perimeter vs. area of clusters, with a sudden jump in perimeter length indicative of fragmentation. When overlaid with US Census bureau data, there was no significant difference between the two areal assessments. This approach was further exploited by Small *et al.* (2005) who used this technique to investigate more general corrections for the overflow phenomenon associated with DMSP-OLS data (see section 3.3.1). The Imhoff *et al.* (1997) analysis applies only to the conterminous United States and it is unknown how this threshold performs in other parts of the world.

Sutton (2003) used the radiance-calibrated data set to investigate urban sprawl in the US, plotting the natural log of lit area vs. the natural log of population for US cities above 50,000. Those cities lying below the regression line were deemed to be affected by urban sprawl since they have a lower population density. Two radiance thresholds were used: the lower one ( $900 \mu\text{W}/\text{cm}^2/\text{sr}$ ) was used to incorporate urban agglomerations, whilst a high one ( $2000 \mu\text{W}/\text{cm}^2/\text{sr}$ ) considered cities more discretely. Cities in the central US were found to have the highest level of sprawl according to this measure.

A synthesized data set of impervious areas (DMSP Data download, 2006) has been produced by NOAA-NGDC, and night-time lights were used to delineate urban areas for CIESIN's Global Rural-Urban Mapping Project (GRUMP) data set (CIESIN 2005).

## 4.2. Population

Population studies have a long history in remote sensing. A review of demographic studies using sources of remote sensing data other than night-time lights and broader methodologies are given in section 5.1 of the CIESIN Thematic Guide to Social Science Applications of Remote Sensing. Population prediction from night-time lights and remote sensing more generally relies on using relationships between the size (area) of a settlement and its population. The allometric growth model has been widely used to model the relationship between area and population. Stewart and Warntz (1958) demonstrated the link between the radius of a built up area and the population living within it. On the basis of their empirical results they established the relationship:

$$r = aP^b$$

where:  $r$  is the radius of a circle of equivalent area to the settlement

$P$  is the Population

$a, b$  are coefficients

The development of aerial photography and remote sensing technology has extended this analysis to regional and global scales.

Initial analysis of night-time light images revealed a striking (though not unexpected correlation) between city-lights and human population density for the continental USA (Sutton *et al.*, 1997). The total area of light at night observed by the DMSP-OLS 'city-lights' product has been observed to correlate with population figures for countries regardless of economic development (Elvidge 1997b; 1997c). Doll (1998) extended these observations to analyse the relationship between the lit-area in a country and urban population. Continent-wide distributions were also examined. Graphs of lit-area versus city population were produced. Lit-area was calculated by converted the lit clusters into polygons using a geographical information system, with the area attached as an attribute to each polygon record. City population and location were collected from a variety of databases including the United Nation's demographic Yearbook for 1995 (UN, 1995), which provided a database for every city with more than 100,000 inhabitants. This resulted in a global database of 2,954 cities with which to compare against the night-time light clusters. The analysis relied on the matching of city locations to clusters of light; both continental and individual country level analysis was performed (Figure 8). Large conurbations often contained multiple population points; in this case, the populations were summed and attributed to the entire lit-area of the polygon. Urban population figures relating to the urban agglomeration rather the city proper were used to be as consistent as possible with the light data. Lit-area versus population relationships were analysed in log-log space as has been advocated in previous studies by Tobler (1969) and Elvidge *et al.* (1997b; 1997c).

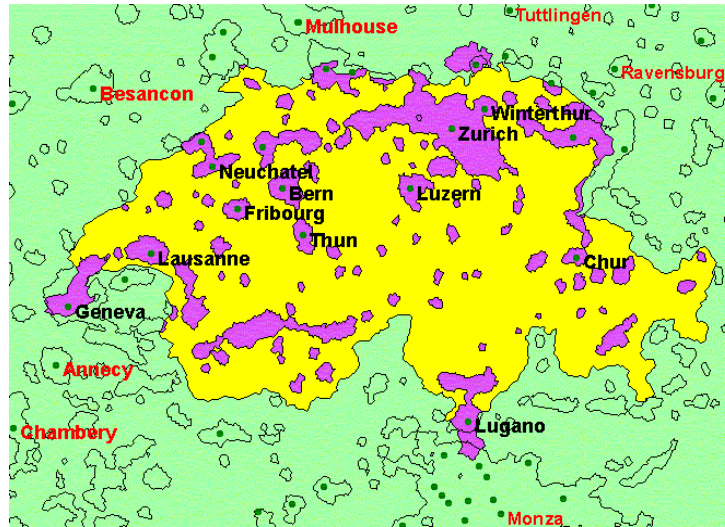


Figure 8. Frequency Composite Image of urban polygons in Switzerland and their associated population points from the database.

At the continental scale the relationship exhibits an essentially linear (in log-log space) distribution, which becomes ever more spread out at lower area/population levels as is shown for Europe in Figure 9. This suggests that the lit area (and presumably population density) varies considerably among small cities and towns. Other error sources contributing to this effect include the inaccurate city population statistics and the assumption that all population is accounted for within the polygon. Care was taken to use the population figures pertaining to the urban agglomeration rather than the individual town where possible.

The individual country relationships tend to be a linear subset of this distribution.

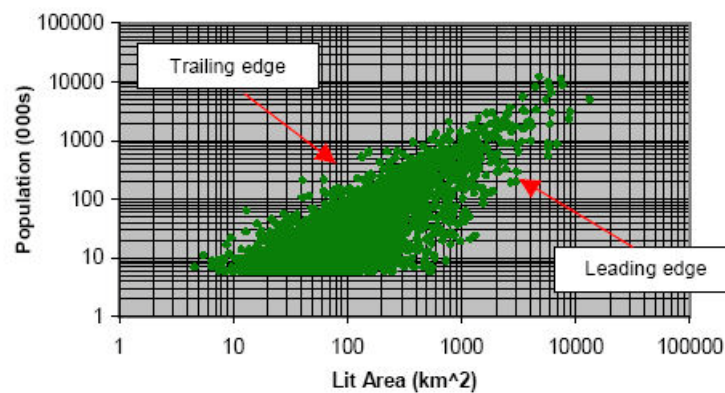


Figure 9. Lit-area/population scatterplot for European cities with annotations referred to in the text below.

The individual country relationships were used to predict the urban population for each country by estimating the population of lit areas which had no population data associated with them. This was then compared to the urban population figure published by the World Resources Institute (WRI, 1996). Forty-six countries were tested in all; these results are presented in Doll *et al.*

(2000). These methods and results were replicated and extended by Sutton *et al.* (2001) who went on to calculate a figure for the global population. This was done by equating this estimated population to the known urban population, and then scaling this up to the total population of a country by using the percentage of people living in rural areas figure. Sutton *et al.* (2001) also observed a broad based distribution to points in his lit-area population scatterplot similar to that shown in Figure 8. These points could be largely resolved by dividing them into three categories based on the per-capita income of the country to which it belonged. Low-income countries (per capita GNP < \$1000) occupied a band of points on the trailing edge of the distribution. Medium income countries (\$1000 < p.c.GNP < \$5000) occupied the middle part of the cluster, whilst high-income countries' points were located further to the right and composed the leading edge. The further to the left of the graph a point is, the smaller the settlement was observed from the night-time light imagery. This implies one of two things: either that the low income countries have the highest population densities, or that much of the population may be undetected due to low lighting in informal settlements

Beyond aerial extent, a more sophisticated use of light-time lights can be employed using the information content (brightness) to ascribe values to population density. Doll and Muller (1999) used the radiance calibrated for country-level population estimation and also investigated population morphology at the city scale in relation to night-time lights (Doll and Muller, 2000). Of note from this study was a spatial mismatch between the location of brightest lights and highest population densities for London. Brightest lights are to be found in downtown areas which tend not to have the highest residential population. Sutton (2003b) explores this further describing a number of functions that may be applied to describe how population density varies as a function of distance from the city center. The models included linear, parabolic, exponential and Gaussian functions to describe the variation in population density from the center to the edge of a cluster. The distance to the edge of a cluster was calculated for each pixel in a cluster. This served as the starting point from which different models could be applied. Pixels over water and/or lying in another country were also evaluated in this way and then discarded to take account of the fact that the highest population density is at the edge of a coast or border for cities like Chicago (Lake Michigan) or Los Angeles (Pacific Ocean). Empirically, the distance grid can be overlaid on to census-block level population density data and then derive a relationship between population density and distance to the center of the cluster. None of these models tested by Sutton (2003) produced a  $R^2$  value greater than 0.30 when tested against the original census. Besides the need for accurate co-registration between the two data sets Sutton (2003b) suggests that varying population density at constant distances from the centre of a cluster is responsible for the low correlation.

Paradoxically, night-time lights may be more indicative of day-time populations since there is a large diurnal migration of people from residential areas to areas of work. Recognition of this concept has been used to create a global database of so-called ambient population by using lights in combination in a wide array of other spatially explicit data. The Landscan database models population globally at 30 arc-minute (~1 km) resolution. Its model aims to allocate population based on where people are likely to be during the day, rather than based on residential location from census data. In order to do this, Landscan takes the census data and redistributes it according to probability coefficients calculated from urban centres, transportation networks, elevation and landcover types (Dobson *et al.*, 2000). There have been annual updates to this methodology since it's creation in 1998, rendering cell-level intercomparison inadvisable. The use of night-time light imagery was subsequently dropped as a model input due to the "overt effect of economic development on the brightness and intensity of lighting" (Bhaduri *et al.* 2002 quoted from Elvidge *et al.* 2007). For access to the data set see Landscan in the References.

Night-time light imagery is also used in the Global Rural Urban Mapping Project (GRUMP), to allocate populations from large census units into urban areas (Balk *et al.*, 2004). This data set of urban areas with coincident population counts has been particularly useful for more precise mapping of populations in larger administrative areas with multiple urban areas whilst essentially preserving the integrity of census data rather than distributing people based on cumulative likelihoods.

As such, the choice of data set will be governed by the application of the study. Landsat offers ambient population counts and high spatial precision although the precise methodology is unpublished, whilst GRUMP offers accurate census (or residential) population mapped using a transparent methodology classified into urban and rural classes.

### 4.3. Economic Activity

The previous section made reference to the mismatch in population and radiance at fine scale resolutions. Given the coincidence of brightest lights and downtown areas which are nodes of economic activity, an obvious extension of the application of night-time lights is to map economic activity.

The relationship between night-time light and economic activity at the country level was first described by Elvidge *et al.* (1997). Using the 1994-95 city lights data set, the lit area was plotted against GDP for a number of countries of varying economic activity. This was subsequently expanded upon by Doll *et al.* (2000), who constructed a global relationship of lit-area vs. GDP and then used this to create the first ever map of disaggregated GDP based on satellite data. This map had a spatial resolution of  $1^{\circ} \times 1^{\circ}$  (geographical coordinates) and estimated the global economy to be worth \$22.1 trillion (1992, international \$, 80% of the total value). Where possible one uses the purchasing power parity (PPP) measure of GDP. PPP attempts to equalize purchasing power across countries so a dollar of PPP GDP should buy the same amount of goods in every country. This is done by analyzing the prices of a basket of goods. It is the standard benchmark for making international economic comparisons.

This result was confirmed and extended by Ebener *et al.* (2005), who used other metrics from the night-time light data set to test correlations with per-capita GDP for application to the targeting of health resources. They found the total and mean frequency of observed lights to be better correlated per-capita GDP than lit-area. Results were grouped by climatic type and the percent of agricultural GDP to improve the relationship, but sub-national estimation was found to be less reliable than national level analysis.

The radiance calibrated data set facilitated the investigation of the relationship between brightness of the lights and GDP rather than lit area. Sutton and Costanza (2002) created a global map of market (and non-market) economic activity at 1km resolution. This employed a similar methodology as used by Doll *et al.* (2000), using a logarithmic relationship between brightness (as opposed to lit-area). There is some concern that this method is not appropriate for mapping across scales greater than one order of magnitude of the input data used to construct the relationship.

In recognition of this limitation, and taking advantage of the existence of better quality economic data for local areas, Doll *et al.* (2006) created maps of the conterminous United States and Western Europe at 5km resolution using linear relationships constructed from sub-national GDP data (Gross State Product for the US). Analysis was carried out on a country by country basis to accommodate the fact that different countries have different relationships based on their cultural

use of lighting. Out of the counties studied the US was found to have highest amount of lighting per unit of economic activity. The use of sub-national data allowed for the analysis of within country differences of the radiance-GDP relationship. In essence, four different types of relationship were identified.

1. Straight linear with all regions lying on a single line
2. Offset outlier where the most economically active area is also the brightest but is anomalously bright compared to other regions.
3. Extreme outlier where the most economically active place is not the brightest area
4. Two relationships in one country, which are geographically separated indicating regional disparity (Figure 10).

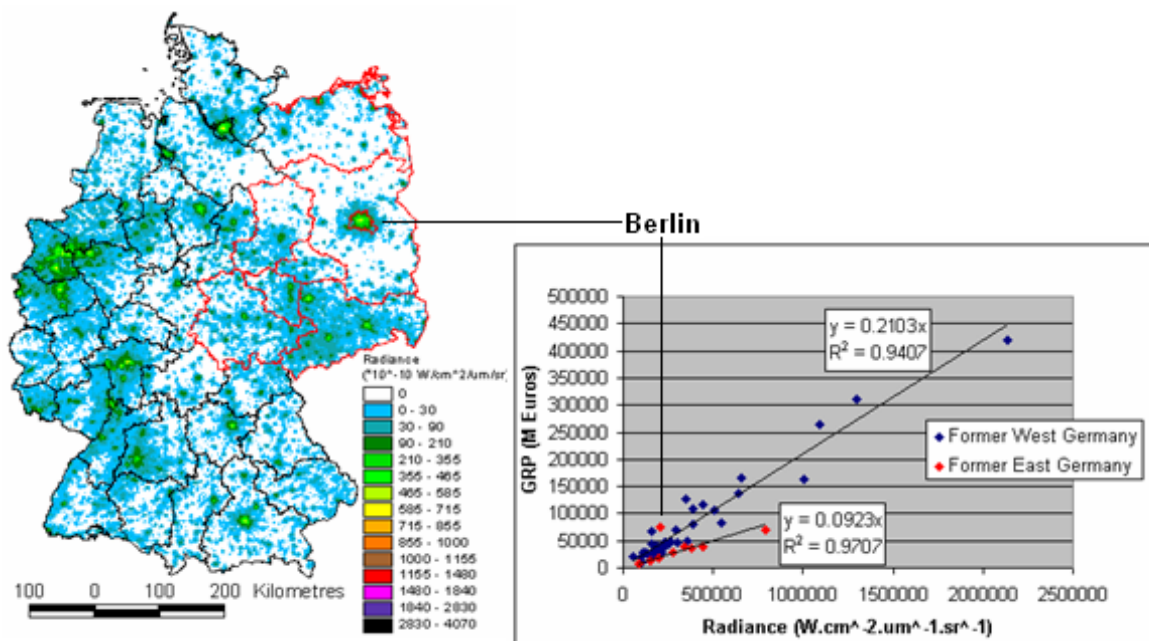


**Figure 10. Light map of Germany and the associated graph of radiance and regional Gross Domestic Product. Note how points in the former East Germany have a different relationship to those in West Germany.**

This analysis has highlighted a number of fruitful research areas to investigate and suggests that lights can offer insights into a range of other areas in the social sciences. Most counties had an outlier of some description, usually with the capital city offset from the other regions in the country. Extreme outliers could also be a function of very small administrative units being used. This suggests that there are some different relationships for the different sectors of the economy.

All these maps use only light to distribute economic activity. This is a reasonable assumption to make in developed countries where industry and service sectors can comprise over 90% of the economy. Although agricultural productivity is spatially more widespread it is represented in these maps as nodes – i.e. the map records the agricultural activity in the towns which emit light, not in the fields where crops are being grown. This is an important caveat to the maps described here and one which would be the first item to address when improving these maps and extending

them into the developing world where agriculture comprises a larger section of the national economy. Agricultural maps produced by the Center for Sustainability and the Global Environment (SAGE) at the University of Wisconsin at Madison are seen as candidate data sets to incorporate with the lights.

An inverse or complementary application of night-time light data is to identify the location of the poor through the absence of light. Elvidge *et al.* (2006) derived a global poverty map by dividing the 2003 lights data set by the 2004 landsat gridded population data set. This was then calibrated to the poverty statistic of the % of people living on \$2 and the relationship used to estimate the poverty count in each grid cell. The total of 2.3 billion people living in poverty compares to 2.6 billion from the World Bank. Whilst there was aggregate agreement at the global level, it was noted that the cultural use of lighting may have led to erroneous results in certain localities; Egypt's poverty estimate of 6.7% was far below its official level of 43.9%, whilst the US states of Vermont and Maine anomalously high estimates could be due to limited outdoor lighting.

Lights by themselves do not adequately capture the full range of economic activity. Other researchers have used different methods to map economic activity, such as applying per capita GDP to population headcounts. This method has other limitations, however, such as the assumption of a uniform level of economic activity and wellbeing across entire populations.

#### 4.4. Greenhouse Gas Emissions

An important policy-relevant area to which night-time lights can make a contribution is that of mapping and monitoring greenhouse gas emissions. Elvidge *et al.* (1997) first identified the correlation between lit area of lights and carbon dioxide (CO<sub>2</sub>) emissions. This was subsequently expanded upon by Doll *et al.* (2000) who investigated mapping CO<sub>2</sub> emissions at 1°x1° resolution in a manner similar to that of economic activity from the same paper. This was compared to a map of CO<sub>2</sub> emissions produced by the Carbon Dioxide Information Analysis Center (CDIAC). Whilst the night-time lights based map did poorly in estimating emissions directly from the relationship, it did a better job of mapping the spatial distribution of emissions. Despite an overall underestimation of emissions, a difference map was produced (Figure 11) and revealed that some areas of the world were overestimated. This is not entirely unexpected as there are some significant outliers in the relationship. In the study by Doll *et al.* (2000), the authors note that many of the former soviet republics appear to have more emissions than would be predicted by the amount of lights present. This is hypothesized to be due to the lower than average level of street lighting and the higher proportion of relatively energy inefficient industrial activities in those countries.

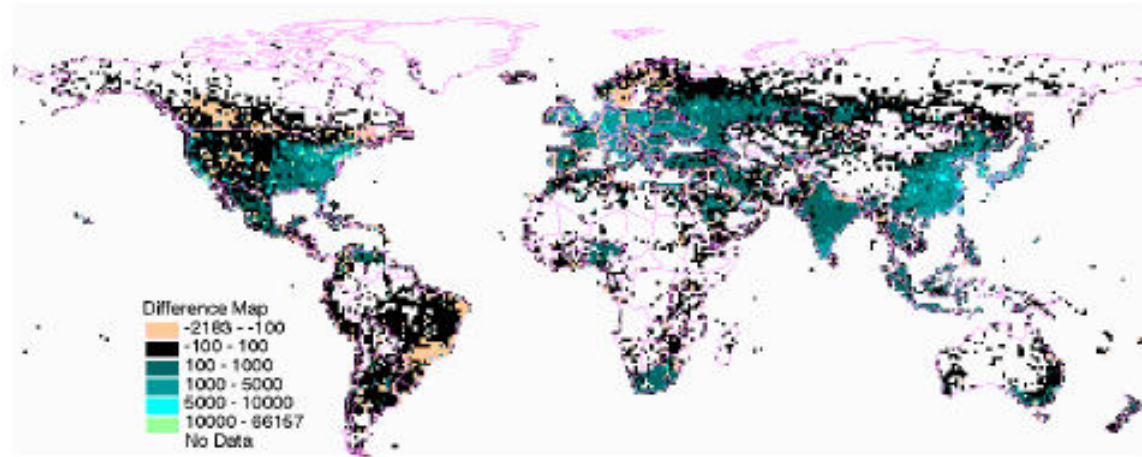


**Figure 11. Difference map between the DMSP-OLS map of emissions and that produced by CDIAC. White areas show the closest agreement between the two maps. Blue areas show where the OLS map over-estimated emissions relative to the CDIAC map, and red areas show where they underestimated them.**

Saxon *et al.* (2000) note that outliers also include small islands states being entirely illuminated. Their small size leads to an extreme concentration of their CO<sub>2</sub> sources, so their emissions are no longer correlated to illuminated area. They go on to discuss how use of the relationship between lights and CO<sub>2</sub> emissions can be used as a benchmarking exercise upon which to base future observations in the model, in order to track country compliance with the Kyoto Protocol – the premise being that starting from an initial starting point, it is possible to track whether a country’s reported emissions reduction is matched by it’s pattern of street lighting and energy consumption.

The poor agreement of the satellite derived CO<sub>2</sub> map with the CDIAC estimates was possibly due to the mode of energy generation (e.g. nuclear, wind, solar) and also how the energy produced was utilised. One has to consider what the ‘invisible’ energy uses are, and how important they are in assessments. The disparate magnitude of emissions between the two maps underlines the requirement for a far more sophisticated model incorporating many more factors than just the relationship between lit-area and emissions. Elvidge *et al.* (2000) described how this might be accomplished using a radiance calibrated night-time lights data set. In the study Elvidge *et al.* presented a graph of cumulative brightness versus energy-related carbon emissions for the 48 conterminous states of the US, which showed the two parameters to be strongly positively correlated. Building on this result, they outlined the extensive ancillary data required to make sensible assumptions about distributing the data. It is likely that countries will also have to be grouped into those which are heavily reliant on fossil fuels, and therefore should have closer agreement to the official estimates. It is also likely that GDP will be a key determinant of how to group these countries, in the same way Sutton *et al.* (2001) has shown for population estimation. Mapping of CO<sub>2</sub> emissions is potentially one of the most valuable applications of using night-time data, if it can be demonstrated to produce reliable and consistent results.

More broadly, Toenges-Schuller *et al.* (2006) used the stable lights data set as a proxy for the pattern of NO<sub>x</sub> emissions (NO<sub>x</sub> emissions are attributable in roughly equal measure to motor vehicles, power generation, and industrial activities). It was used in conjunction with an emissions inventory database, which provided source strength data and a global 3D chemical transport model (CTM), which simulates the mixing ratios for 63 chemical species. The lights

were converted into NO<sub>x</sub> emissions by integrating over lit pixels falling in the larger grid of their CTM. Using the light data made the assumption that there was no annual variability. This was then compared to measurements taken from dedicated satellite sensors measuring atmospheric NO<sub>x</sub> concentrations. In this study the lights were used as an independent verification for measurements taken from another satellite sensor rather than as a direct proxy for a variable, which would then need to be validated.

As with economic activity, lights only partially capture the magnitude and distribution of greenhouse gas emissions. Whilst city lights may act as proxy for general/aggregate diffuse emissions, more specific information would include the locations of the densest air routes and a comprehensive database of power station locations to properly identify point source emissions. One component of point source emissions where lighting is specifically generated comes from gas flaring. Gas flaring occurs at petroleum production and processing facilities, where the gas by product is safely burnt off. These show up as very bright circular clusters on night-light imagery. Elvidge *et al.* (2007) used a time series of images to quantify the amount of gas flaring occurring globally between 1995-2006 as part of the Global Gas Flaring Reduction Initiative. Countries were found to follow 4 main trends, stable; experiencing a downward trend; increasing trend over time whilst others peaked in the middle of the time series. However, they found an aggregated stabilized pattern of flaring at the global level ranging between 150-170 Billion cubic meters/year over the period of observation.

#### 4.5. Light Pollution

Probably the most intuitive application of night-time data is to map and quantify the amount of light pollution. A clear view of the universe serves as a constant reminder to consider the nature of our existence and begs questions which we may never be able to answer. However, a clear view of the night sky for those who live in the developed world is a rarity.

Cinzano *et al.* (2001) set about using the DMSP-OLS radiance-calibrated night-time light data set to quantify artificial night sky brightness. Light propagation from the top of the atmosphere radiances present in the DMSP-OLS product was modelled through Rayleigh scattering by molecules, Mie scattering by aerosols, atmospheric extinction along light paths, and Earth curvature. Hence, many areas that should appear dark in the night-time light product due to the absence of a ground level light source are in fact affected by light pollution from adjacent bright areas. Cinzano *et al.* (2001) intersected their atlas of light pollution with the Landsat 2000 global population density database (Dobson *et al.* 2000) to assess the number of people affected. The extent of this pollution is so widespread across the developed world that more than 99% of the population of the European Union and United States and 66% of the entire world population suffer from some degree of light pollution. In particular, about half the population of the developed world does not have the possibility of viewing the Milky Way with the naked eye.

The MANTLE project (Mapping Night-Time Light Emissions) was an EU funded project conducted among eight European academic and private bodies. Using the DMSP-OLS radiance-calibrated data set as its primary data source, it aimed to investigate how it can be used as a surrogate for a range of socio-economic indicators including GDP, population, energy consumption, urban typology, and landscape/skyscape quality. Using GIS-based modeling techniques, they developed a means of modeling light pollution by land cover classes to enhance the night-time light data set (Figure 12). Combining such enhanced data with other spatially

explicit urban data such as road networks may be used to create environmental disturbance maps and their counterparts, tranquility maps.

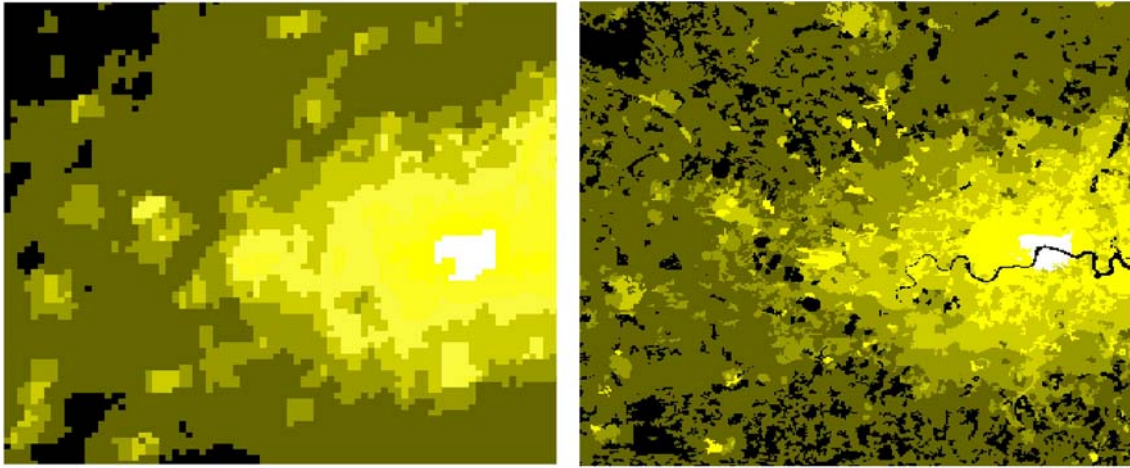


**Figure 12. Result of using landuse classes to enhance night-time lights with the original DMSP-OLS image on the left and the result of its enhanced light pollution map based on land cover classes.**

Besides obscuring the night sky, nocturnal lighting affects species across all taxonomic groups in urban and other ecosystems. The primary modification to species behaviour is that it attracts many insects, which in turn attracts its prey. Bats are a good example of how their traditional predatory instincts are affected by their prey becoming more spatially concentrated around street lamps (Rich and Longcore 2006). The reason why fishing fleets can be detected in DMSP-OLS imagery is because the fishermen use powerful lamps to attract squid to the surface waters. Other impacts include increased predation of sea turtle hatchlings (Salmon et al. 2000, Salmon 2006) and mortality of seabirds attracted to offshore gas flares (Wiese et al. 2001, Montevecchi 2006). Declining reptile populations and changes in lacustrine zooplankton have also been noted (Moore et al, 2001). However such effects are as yet largely unquantified due to the coarse resolution of the OLS sensor and problems with overglow. Nonetheless, scotobiological research could be greatly advanced if improvements to these parameters are made (see section 5.3; see glossary for definition of scoto-biology).

Whilst lights have largely unintended effects of species behaviour, the deliberate use of lights to attract species is via powerful lamps to attract squid to the ocean surface is well captured from DMSP-OLS imagery. Walluda *et al.* (2004) described a study using night-time lights data to quantify the size of fleets fishing the jumbo flying squid (*Dosidicus Gigas*) in the Eastern Pacific off the coast of Peru. Orbital DMSP-OLS data (as opposed to annual composite) for July to December was compared to satellite based ship data in order to calibrate the illuminated area to the size of the fishing fleet. A correction was applied for the considerable reflection from the sea surface. They were able to estimate the size of fleets to within 2 vessels 83% of the time suggesting it maybe a useful tool to police certain fisheries and encroachment into Exclusive Economic Zones. Further effects of lighting on species are discussed in section 5.3.

Another marine application has used night-time lights to assess anthropogenic stress to coral reefs, which is a highly sensitive component of the marine ecosystem. In this case, it is not the precise location of the lights themselves, but the relative location of light to the reef that is

important. Aubrecht *et al.* (2008) presented a method which evaluates the proximity of cities, boats and gas flares using thresholds of 25km, 5km and 5km respectively for each class. The lights index (pixel DN divided by cloud-free frequency of observation) of the 2003 night-time lights annual composite was used in this study to calculate a light proximity index (LPI) by summing the quotient of pixel values and respective distance for each reef location. The study is of interest to this guide as it provides a useful overview of the different considerations researchers seeking to use these data in any analysis would do well to think about:

- i) Data collection and algorithm design based on the format of the respective datasets. In this example reefs could be treated as either individual entities or aggregated to the level of the entire reef group. *How to assimilate disparate datasets to answer your research question?*
- ii) The choice of threshold distance for different classes and how to calculate the impact of light on coral reefs. A linear distance decay model was used but other formulations are available. *What is the basis for choices in the model?*
- iii) Analysis of results. Aubrecht *et al.* (2008) consider total LPI and then mean LPI for the number of points in a reef cluster. In such a ranking small reef systems with few points may be over emphasized at the expense of larger ones. Splitting the light emissions by source allows reef stress from different sources to be identified as areas suffering from multiple stressors. *Sensible design allows for flexible analysis.*
- iv) Interpretation of results. Their analysis shows that coral reefs around Singapore are the most stressed, however this is a relatively small coral reef. An alternative interpretation might decide that a larger reef group with a lower average LPI is at higher risk because it plays a greater role in the marine ecosystem at that location. *How do you relate satellite derived indicators back to the phenomenon being studied?*

The full list of reefs and associated LPI values are available from the DMSP data download site.

The issue of light pollution has become an increasingly popular cause, with a recent *National Geographic* article (Klinkenborg, 2008) and the growth of the International Dark-Sky Association. Concern arises from the effects on wildlife and on human societies, as people become increasingly disconnected from nature and the universe around them due to the blotting out of the night sky by inefficient lighting. Night-time light data will be an important way to monitor where night skies are becoming more polluted by increases in lighting, or where there are declines in light pollution due to economic factors or improvements in light direction and efficiency.

#### 4.6. Disaster Management

The observation of light (or its absence) offers the potential to monitor urban areas after in the wake of a disaster or fires in rural areas, Damage to street lights, buildings or power stations or power lines can all result in the lower levels of light being detected after a large-scale catastrophe has occurred. The following case studies highlight how DMSP-OLS data may be used to quantify and direct recovery. As with all optical remote sensing systems, this relies on the absence of cloud cover.

The identification of fires from satellite imagery is facilitated due to their distinct spatial (non-urban) and temporal features. Biomass burning can be identified in forest areas by lights which

have a short temporal duration. Aside from their location, gas flares have a limited spatial extent and are extremely bright. Elvidge *et al.* (2001b) used DMSP-OLS data to assess the areal extent of biomass burning in Roraima, Brazil, whilst other studies have sought to establish relationships between the thermal properties of the fire, the rate of biomass consumption (fuel load), and aerosol and trace gas emissions also from satellite data (Kaufman *et al.* 1998). These figures are not currently included in estimates of CO<sub>2</sub> emissions.

Kiran Chand *et al.* (2006) used DMSP-OLS data to detect fires and compare it with other satellite based fire detection methods. Night-time light imagery can provide useful supplemental information for fire detection since it uses different image information (light rather than temperature). The enhanced sensitivity of the OLS instrument means it can detect a flame front an order of magnitude smaller (~ 45m<sup>2</sup>) than AVHRR or MODIS (Cahoon *et al.*, 2000). Kiran Chand *et al.* (2006) developed a fire detection algorithm for the DMSP-OLS sensor which involved analyzing pixels from individual overpasses which lay outside the stable lights data set. These were then compared the results to those from the MODIS fire product and also from the Indian AWiFS satellite, which is similar in specification to Landsat (multispectral, 56m resolution). Good agreement (98%) was found between DMSP and the other satellite based measurements, when comparing detected fires with burnt areas. The use of night-time imaging for fire detection provides a valuable contribution to satellite based fire detection in that it helps the identification of the most destructive fires; namely those which extend from one day to the next and are thus detectable at night.

A number of studies have examined the use of night-time lights to assess affected areas in disaster situations. As with fire detection, the basis of the method involves the comparison of a single overpass with the longterm known presence of lights. Figure 13 shows the extent of light disruption in Mississippi and Louisiana following hurricane Katrina in September 2005.



Figure 13. Affected area (show in red) of blacked out lights during hurricane Katrina with the 2004 Annual Composite vs. August 30, 2005 local time on the left and the 2004 Annual Composite vs. Sept. 11th local time on the right.

Kohiyama et al (2004) described how DMSP-OLS data is used in a disaster information system to provide near-real time early damaged area estimation. Using either two or a time-series of images, they applied significance tests based on the observed lights compared to the lights prior to the disaster event. The assumption used is that under 'normal' conditions the changes in brightness of city lights follow a Gaussian distribution. Their system EDES (Early Damaged-Area Estimation System) is currently the only known operational use of night-time light imagery for disaster assessment.

De Souza-Filho *et al.*, (2004) monitored Brazil's energy crisis in 2001 with DMPS-OLS data. Using data collected in 2000 and 2001, they compared a dip in Electrical output over the Federal District in Brazil 2001 with a changes in brightness from the previous year, For this limited study they found good agreement with a coincident drop in energy consumption and brightness of around 20%.

## 5. Other sources of current and future night-time light data

The DMSP-OLS sensor is currently the only space borne sensor imaging settlements at night on a consistent and regular basis. However, there are other means of acquiring night-time imagery over cities. This section deals with three other attempts to take imagery of cities at night. The first is from the astronauts aboard the International Space Station, who achieve stunning results using a handheld camera looking out of the portholes. Secondly, results are reported from dedicated airborne missions flown by NASA using both low light imagers and hyperspectral imagery. The results of these experiments inform the third and final section of this guide, namely the desired attributes for a future mission to capture night-time imagery over cities. This section will discuss the typical trade-offs all remote sensing satellites face: period of return, wavebands, spatial resolution in the context of a proposed mission to continue imaging our urban environments at night.

### 5.1. Astronaut photography

The only other space borne source of night-time light imagery comes from the astronauts aboard the International Space Station (ISS). Using a handheld camera Kodak DSC 760 camera, it has been possible to generate some stunning views of cities at night. All crews have attempted night-time light photography over cities at night, however the results are variable and often produced blurred city light imagery. This was substantially improved thanks to a tracking device built out of equipment on the ISS by one crew member, Don Petit. He practiced several hours to get the quality of imagery available from ISS006. Unfortunately, since this tracker takes a long time to learn to use, subsequent crews have not reassembled it (Stephanov, 2006).

Astronaut satellite imagery can be accessed from their gateway to astronaut photography (NASA, 2007). The crispest images are from collection ISS006, when Don Petit was flying aboard the ISS. There are hundreds images of cities at night from every region in the world. A searchable file of this collection is available here.

Nonetheless, requests for imagery can be made. However, there are a number of uncontrolled variables which affect dedicated image acquisition. These include the astronauts' awake period (typically 6:00-21:30 GMT) during which time they can obtain imagery, the precessing nature of the ISS orbit that governs which areas of the Earth are visible at a given time and cloud cover over the target area. Essentially, we would have to wait until these conditions were optimal before attempting to acquire useful images. The astronauts themselves would also need some training time, as their usual targets are acquired with full solar illumination.

Further drawbacks to astronaut imagery include.

- There is no precise geolocation information beyond the centre coordinates to a half decimal degree precision.
- The images are taken by hand
- There is no consistent spatial resolution to the imagery (estimated to be 6m/pixel)
- Brightness differences can only be interpreted in a qualitative sense.

However, when viewed in comparison to the DMSP-OLS sensor one can instantly see the detail, which the OLS sensor is heavily obscuring. Much research has been conducted over the Las Vegas area. In the two panels (Figure 14) we see the DMSP-OLS image of Las Vegas from the 2003 with an image taken from the ISS. We see the strip is clearly visible and very bright, as are major highways, whilst the rectilinear layout of the city is also clearly identifiable.

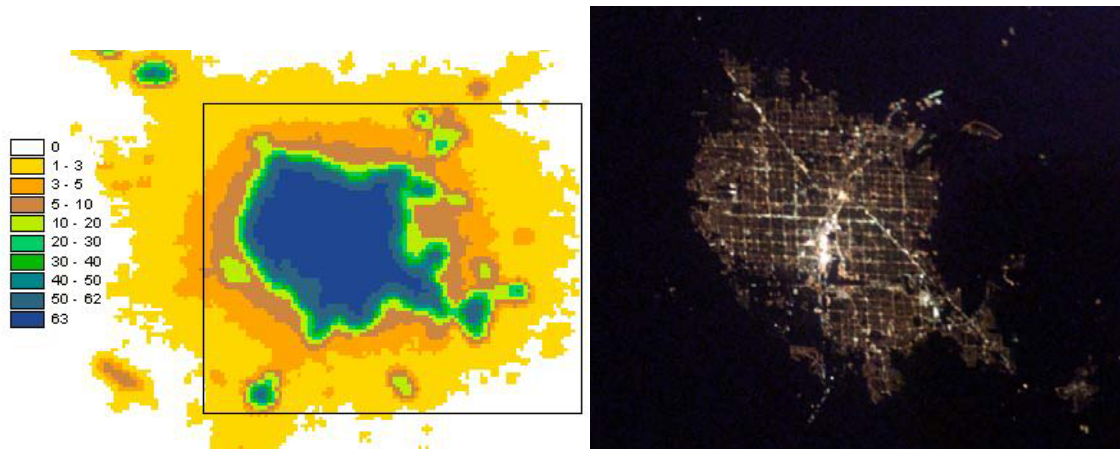


**Figure 14. Comparison of DMSP-OLS average DN image for 2003 over Las Vegas (left) and one taken from the International Space Station on April 7<sup>th</sup> 2003 at 9.13pm local time (right: Image courtesy of NASA-JSC). The black box indicates the estimated extent of the ISS image in the OLS scene.**

Nonetheless, it is possible for skilled remote sensing analysts to use this imagery should sufficient tie points be established with other remote sensing/aerial photograph or map data to identify ground locations and warp the image to other data sources. The author has investigated its use for disaster response management in the aftermath of hurricane Katrina in 2005. This was unsuccessful primarily due to the absence of cloud free overpasses of New Orleans and the time needed for the crew to familiarize themselves with the tracking device.

## 5.2. Dedicated airborne missions

In the absence of space borne sensors, researchers have used sensors mounted on aircraft to fly high altitude missions. The Airborne Visible/Infrared Imaging Spectrometer (AVIRIS) is one such sensor that may be used to acquire high-resolution data over individual cities at night. The AVIRIS sensor is a hyperspectral imaging system that senses in 224 very narrow bands (~10nm) from 0.41-2.45  $\mu\text{m}$ . It is designed to fly onboard NASA's U2 aircraft where, at an altitude of 20km, it can image 20m pixels over a 10km wide swath (Porter and Enmark, 1987). This additional data source offers not only the advantage of an enhanced spatial resolution, but also of enhanced spectral resolution too. AVIRIS data could address this issue. A test flight over Las Vegas in 1998 suggested that there are distinctive spectral signatures over the city (Elvidge and Jansen, 1999; Doll, 2003). Combining these two data sources would be of use to help understand what the DMSP-OLS data is really showing at the small scale, and therefore aid the assumptions one makes in macro-scale models using nighttime imagery. There are various types of lighting used in cities. Each has distinct spectral characteristics depending on the element used. Commonly used types of high intensity discharge lights are high pressure sodium used for street

lights, mercury vapour and metal halide used in lighting car-parks and sports stadiums. Mapping spectral patterns over cities could help to identify patterns of residential, commercial and industrial land-use (Elvidge and Jansen, 1999). This could be one way of filtering out the population component if concerned with assessing areas of high economic activity.

More recently, imagery has been taken over Las Vegas as part of specification identification mission for proposing a new night-time light satellite. Figure 15 shows a scene taken over the main strip in Las Vegas and compares it to conventional daytime high resolution satellite data. The spatial resolution is around 1.5m for the night-time imagery. Individual lamps can be seen in parking lots behind the Monte Carlo and Alladin hotels. Dark areas include golf courses and the airport in the bottom right, the main runway isn't lit although the aircraft stands are illuminated. The Luxor hotel is famous for a bright beam of light projected out through the top of the pyramid causing the sensor to saturate in this location. At this high resolution it is clear that outline of many distinctively shaped buildings in the area due to lighting used to illuminate their façades.

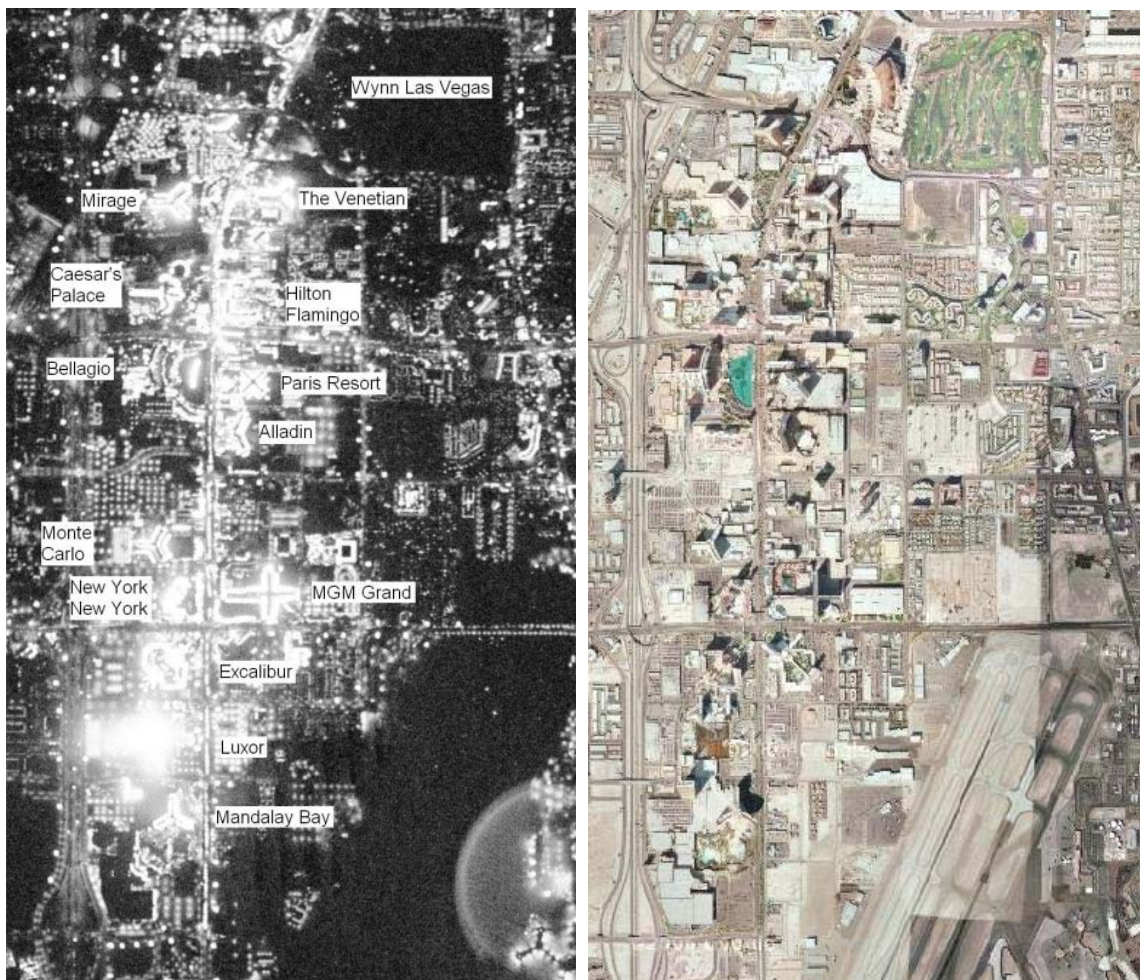


**Figure 15. Comparison of Las Vegas strip view from night-time ER-2 plane and the corresponding daytime scene.**

Airborne data provides a means for taking imagery at a high spatial resolution with high quality metadata concerning the camera model, calibration and geolocation of the imagery than would be

available with astronaut imagery. The drawback is however, that it is costly to the user to obtain and little to none of it is publicly available. Samples of Hyperspectral AVIRIS imagery together with samples of night-time Landsat imagery is available from NOAA-NGDC. See the Other Night-time Data section of the DMSP Data Download in the References.

### 5.3. Nightsat Mission

Given these recent developments and experiments with higher resolution airborne remote sensing and our existing knowledge from working with the DMSP-OLS instrument, what would be the desired set of attributes for a new dedicated night-time light sensor?

A proposal submitted to NASA has outlined these parameters. Many of the orbital parameters are a function of choosing the spatial resolution and swath of the sensor. Titled Nightsat, the instrument would have the following characteristics.

The spatial resolution is recommended to be 25-50m. Based on experiments resampling the 1.5m Cirrus imagery, this was determined to be the maximum resolution permissible for delineating primary night-time lighting patterns. At this resolution and a swath of 80-90km, there would be a revisit period of ~30 days, at the equator yielding 12 views per year. The overpass pass time would be 9.30pm local time to provide the temporal consistency for change detection. As with DMSP, cloud and fire screening would be done with a separate thermal band. A key feature would include on-board calibration or a repeatable procedure for calibrating sensor data to radiance units and allow comparisons over time and between future sensors.

There are essentially three types of lights which are detected: Flames such as lanterns and gas flares; Incandescent, where light is produced from a heated filament; and vapour lamps where lighting is generated by electrically charged gasses such as mercury, sodium and neon. Incandescent and vapour lamps are most common for outdoor lighting. Each type of light has a distinctive spectral signature (Figure 16), which would be detectable if the new satellite had four band multispectral sensor to define the predominant type or mixture of lighting present.

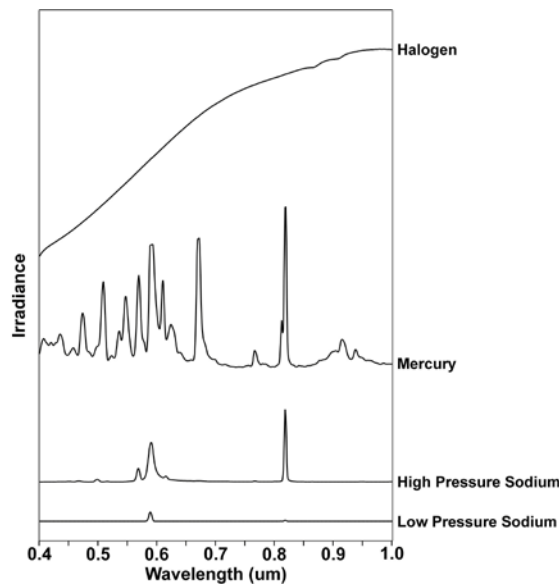


Figure 16. Field spectra of four different types of nocturnal lighting.

The ability to distinguish different types of lighting will have benefit for a number of applications. Classifying urban land use the use of different types of light is one promising area, especially as lighting practices tend to be homogeneously determined at some municipal, regional or even national scale.

For ecological applications, the presence of certain wavelengths determines whether species will respond to lights or not. Sea turtle nesting and seafinding behaviors are not affected by lights with only yellow wavelengths (Lohman *et al.* 1997, Salmon 2006), whilst salamanders and some birds show difficulty to navigate under certain lighting conditions. Some salamanders are unable to navigate properly under yellow light (Wise and Buchanan 2006; Wiltchko and Wiltchko 2002), while insects are attracted to short, ultraviolet light (Frank 1988).

Beyond this, high resolution night-time light imagery has the potential to answer social questions hitherto unconsidered in any scientific manner. For instance, one could test the widespread belief that nighttime lighting deters crime. Very few studies have been able to evaluate the effectiveness of lighting in varying settings and over time (Weeks, 2003), but combining night-time light data with data on crime and socio-economic and demographic characteristics could inform policy makers and police forces on efficient use of their resources.

## Glossary of Terms

**DMSP-OLS** - Defense Meteorological Satellite Program (DMSP) Operating Linescan System (OLS). The OLS is the sensor which detects lights at night. It flies aboard the DMSP platform. Multiple sensors can fly on one platform.

**DN** – Digital Number, a positive integer assigned to response of a sensor relative to the intensity of the signal received by the sensor. Depending on the number of bits assigned to the quantifying sensor response this is usually 6-bit  $2^6 = 64$  (0-63) or 8-bit  $2^8 = 256$  (0-255). The radiance calibrated night-time lights have 8-bit quantization, the average DN product has 6-bit quantization.

**Gain** - The term for the amplification applied to a detected signal at the sensor. Commonly expressed as the ratio of the signal output to the system input. Expressed in decibels (dB), the log of amplification.

**GDP** - Gross Domestic Product. The market value of all final goods and services produced within a country in a given period of time. There are a number of ways this can be calculated, which theoretically give the same value. For international comparisons the purchasing power parity (PPP) measure is used as opposed to the market exchange rate (MER)

**GHG** - Greenhouse Gas Emissions. The term applied to those gases in the Earth's atmosphere which contribute to the greenhouse effect, which are emitted through human activity. Naturally occurring greenhouse gases include water vapor, carbon dioxide, methane, nitrous oxide, and ozone. Certain human activities, however, add to the levels of many of these naturally occurring gases.

**NOAA** - National Oceanic and Atmospheric Administration. Organisation responsible for the DMSP satellite series.

**NGDC** - National Geophysical Data Center, Division of NOAA based in Boulder, Colorado.

**Pixel Saturation** - When a sensor detects a signal which exceeds the dynamic range of a sensor, the sensor records the maximum value. The pixel under considerations is said to be saturated. There is no way of determining the strength of the signal once saturation occurs

**PPP** - Purchasing Power Parity. The standard for international comparisons of GDP. The PPP attempts to account for market exchange rate distortions by taking the drawing comparisons of prices from a basket of commonly used equivalent goods.

**Scotobiology** - The study of biology as directly and specifically affected by darkness. (scoto from the Greek, darkness).

**Specular Reflectance** - That component of the light reflecting from a surface caused by its shiny or glossy nature. Shiny surfaces reflect light striking them in clearly defined angles of incidence, resulting in "hot spots" corresponding to the direction of the light sources providing the illumination.

**Total DN** – The sum of all digital numbers in a given region. In the context of night-time lights (and the absence of radiometric calibration), total DN is used as a proxy for total brightness of a region.

## Figure Credits

Figure 1. Source: Air Force Research Laboratory Space Vehicles Directorate.

Figure 2. Images created by Chris Doll. Derived from three different data sets (from left to right: Stable Lights, Radiance Calibrated, and Average DN) derived from Version 2 DMSP-OLS Nighttime Lights Time Series.

Figure 3. Images created by Chris Doll using data set: Version 2 DMSP-OLS Nighttime Lights Time Series. F15. 2002.

Figure 4. Images created by Chris Doll using data set: Version 2 DMSP-OLS Nighttime Lights Time Series. F10. 1992; F12. 1998; F15. 2003

Figure 5. Graph created by Chris Doll using data sets: Version 2 DMSP-OLS Nighttime Lights Time Series. F12. 1997; Version 2 DMSP-OLS Nighttime Lights Time Series. F14. 1997.

Figure 6. Graph created by Chris Doll using data sets: Version 2 DMSP-OLS Nighttime Lights Time Series. F12. 1997; Version 2 DMSP-OLS Nighttime Lights Time Series. F14. 1997.

Figure 7. Images created by Chris Doll using data sets: Version 2 DMSP-OLS Nighttime Lights Time Series. F12. 1994; Version 2 DMSP-OLS Nighttime Lights Time Series. F12. 1995; Version 2 DMSP-OLS Nighttime Lights Time Series. F12. 1996; Version 2 DMSP-OLS Nighttime Lights Time Series. F12. 1997; Version 2 DMSP-OLS Nighttime Lights Time Series. F12. 1998; Version 2 DMSP-OLS Nighttime Lights Time Series. F12. 1999.

Figure 8. Images created by Chris Doll using data set: Polygon outlines of 1994-95 Stable lights, with ESRI GIS national boundary layer and city points from World Urban Centers Database held by the University of Iowa's Center for Global and Regional Environmental Research. Image reproduced from Chris Doll (dissertation 2003). Also need to reference dissertation in the Reference section.

Figure 9. Graph created by Chris Doll using World Urban Centers Database held by the University of Iowa's Center for Global and Regional Environmental Research, supplemental population data from Philip's Geographical Digest 1998-99, plotted against areas derived from the 1994-95 Stable lights data product over Europe. Graph reproduced from Chris Doll (dissertation 2003). Also need to reference dissertation in the Reference section.

Figure 10. Images created by Chris Doll using data set: 1996-97 Radiance Calibrated DMSP-OLS Dataset, graph constructed with values from this dataset and sub-national GDP data for 1997 from Eurostat. Image reproduced from Chris Doll (dissertation 2003).

Figure 11. Image created by Chris Doll using map created from 1994-95 DMSP-OLS dataset and CDIAC gridded CO<sub>2</sub> emissions (ndp058).data set: DMSP-OLS ? Image reproduced from Chris Doll (dissertation 2003). Also need to reference dissertation in the Reference section.

Figure 12. Images reproduced from MANTLE EPROS 2003 Presentation available from: [http://forum.europa.eu.int/Public/irc/dsis/radstat/library?l=/epros-2004/presentations\\_previous&vm=detailed&sb=Title](http://forum.europa.eu.int/Public/irc/dsis/radstat/library?l=/epros-2004/presentations_previous&vm=detailed&sb=Title)

Figure 13. Image and data processing by NOAA's National Geophysical Data Center, Earth Observation Group, Boulder, CO. <http://www.ngdc.noaa.gov/dmsp>  
DMSP data collected by US Air Force Weather Agency.

Figure 14. Image on left created by Chris Doll using data sets: Version 2 DMSP-OLS Nighttime Lights Time Series. F15. 2003. Photograph on right from NASA Johnson Space Center database of astronaut photography.

Figure 15. Remote sensing image on left from Chris Elvidge. Image on right from Google Maps.

Figure 16. From Elvidge et al. 2007b.

## References

- Aubrecht, C., C.D. Elvidge, T. Longcore, C. Rich, J. Safran, A. E. Strong, et al. 2008. A global inventory of coral reef stressors based on satellite observed nighttime lights. *Geocarto International*, Volume 23, Issue 6 December 2008 , pages 467-479.
- Balk, D., Pozzi, F., Yetman, U. and Nelson, A. (2005). The Distribution of People and the Dimension of Place: Methodologies to Improve the Global Estimation of Urban Extents. *International Society for Photogrammetry and Remote Sensing Proceedings of the Urban Remote Sensing Conference*, Tempe, AZ, March 2005.
- Bhaduri, B., Bright, E., Coleman, P., and Dobson, J. *LandScan: Locating people is what matters. Geoinformatics 2002*; 5; 34-37
- Cahoon Jr., D.R., Stocks, B.J., Alexander, M.E., Baum, B.A., and Goldammer, J.G. 2000. Wildfire detection from space: Theory and application. Biomass burning and its inter-relationship with the climate system. *Advances in Global Change Research*. 151-169.
- Cinzano, P., Falchi, F. and Elvidge, C.D., 2001. The first world atlas of the artificial night sky brightness. *Monthly Notices of the Royal Astronomical Society*, 328 (3), 689-707.
- Croft, T.A., 1978, Nighttime images of the Earth from space. *Scientific American*, 239, 68-79.
- de Sherbinin, A., Balk, D., Yager, K., Jaiteh, M., Pozzi, F., Giri, C., and Wannebo, A. (2002). Social Science Applications of Remote Sensing. A CIESIN Thematic Guide. Available at [http://sedac.ciesin.columbia.edu/tg/guide\\_main.jsp](http://sedac.ciesin.columbia.edu/tg/guide_main.jsp)
- Dobson, J.E., Bright, E.A., Coleman, P.R., Durfee, R.C. and Worley, B.A., 2000. LandScan: A global population database for estimating populations at risk. *Photogrammetric Engineering and Remote Sensing*. 66 (7), 849-857.
- Doll, C.N.H, Muller, J-P., and Morley, J.G. 2006. Mapping regional economic activity from night-time light satellite imagery. *Ecological Economics*. (57) 75-92
- Doll, C.N.H. 2003. Understanding the information content of night-time light satellite data for modelling socio-economic dimensions of global change. Ph.D. Thesis. University of London.
- Doll, C.N.H. and J-P Muller., 1999a. An evaluation of global urban growth via comparison of DCW and DMSP-OLS satellite data. In: *Proceedings of IEEE International Geoscience and Remote Sensing Symposium (IGARSS'99)*. Hamburg, Germany 28 June – 2 July. 1134-1136.

- Doll, C.N.H. and Muller, J-P., 1999b. The use of radiance calibrated night-time imagery to improve remotely sensed population estimation. In: Proceedings of the 25th Annual Conference of the Remote Sensing Society. University of Wales, Cardiff, UK 9-11 September. Nottingham, UK: Remote Sensing Society, 127-133.
- Doll, C.N.H. and Muller, J-P., 2000. A comparison of different techniques applied to the UK to map socio-economic parameters: implications for modelling the human dimensions of global change. In: International Archives of Photogrammetry and Remote Sensing, GISC bv: Amsterdam, The Netherlands, 33 (B4), 222-229.
- Doll, C.N.H., 1998. Assessing the potential for quantitative estimation of socio-economic parameters from DMSP-OLS imagery. Dissertation (MSc). University of London.
- Doll, C.N.H., 2003. Estimating non-population parameters from night-time satellite imagery. In: Mesev, V. (Ed.) Remotely Sensed Cities. Taylor & Francis: London, UK, 335-354.
- Doll, C.N.H., Muller, J-P. and Elvidge, C.D., 2000. Night-time imagery as a tool for global mapping of socio-economic parameters and greenhouse gas emissions. *Ambio*, 29 (3), 157-162.
- Ebener, S., Murray, C., Tandon, A., and Elvidge, C. 2005 From wealth to health: modeling the distribution of income per capita at the sub-national level using nighttime lights imagery. *International Journal of Health Geographics*, 4:5.
- Eidenshink, J.C. and Faundeen, J.L., 1994. The 1km AVHRR global land dataset - 1st stages in implementation. *International Journal of Remote Sensing*. 15 (17), 3443-3462.
- Elvidge, C. D., Cinzano, P. Pettit, D.R., Arvesen, J., Sutton, P., Small, C., Nemani, R., Longcore, T., Rich, C., Safran, J., Weeks, J. and Ebener, S. (2007b). The Nightsat mission concept. *International Journal of Remote Sensing* 28 (12). 2645-2670.
- Elvidge, C.D. and Jansen, W.T., 1999. AVIRIS observations of nocturnal lighting. AVIRIS Airborne Geosciences Workshop Proceedings, JPL. Available from: [http://popo.jpl.nasa.gov/docs/workshops/99\\_docs/16.pdf](http://popo.jpl.nasa.gov/docs/workshops/99_docs/16.pdf)
- Elvidge, C.D., 2002. Global observations of urban areas based on nocturnal lighting. *LUCS Newsletter*, 8, 10-12.
- Elvidge, C.D., Baugh, K.E., Dietz, J.B., Bland, T., Sutton, P.C. and Kroehl, H.W., 1999. Radiance calibration of DMSP-OLS low-light imaging data of human settlements. *Remote Sensing of Environment*, 68 (1), 77-88.
- Elvidge, C.D., Baugh, K.E., Hobson, V.R., Kihn, E.A., Kroehl, H.W., Davis, E.R. and Cocero, D., 1997b. Satellite inventory of human settlements using nocturnal radiation emissions: A contribution for the global toolchest. *Global Change Biology*, 3 (5), 387-
- Elvidge, C.D., Baugh, K.E., Kihn, E.A., Kroehl, H.W. and Davis, E.R., 1997a. Mapping city lights with nighttime data from the DMSP operational linescan system. *Photogrammetric Engineering and Remote Sensing*, 63 (6), 727-734.
- Elvidge, C.D., Baugh, K.E., Kihn, E.A., Kroehl, H.W., Davis, E.R. and Davis, C.W., 1997c. Relation between satellite observed visible-near infrared emissions, population, economic activity and electric power consumption. *International Journal of Remote Sensing*, 18 (6), 1373-1379.
- Elvidge, C.D., Baugh, K.E., Tuttle, B.T., Howard, A.T., Pack, D.W., Milesi, C. and Erwin, E.H. (2007a). A Twelve Year Record of Natural Gas Flaring Derived From Satellite Data (submitted to *International Journal of Energy Research*).
- Elvidge, C.D., Hobson, V.R., Baugh, K.E., Dietz, J.B., Shimabukuro, Y.E., Krug, T., Novo, E.M.L.M. and Echavarria, F.R., 2001b. DMSP-OLS estimation of tropical forest area impacted by surface fires in Roraima, Brazil: 1995 versus 1998. *International Journal of Remote Sensing*, 22 (14), 2661-2673.
- Elvidge, C.D., Hobson, V.R., Nelson, I.L., Safran, J.M., Tuttle, B.T., Dietz, J.B., and Baugh, K.E. 2003. Overview of DMSP OLS and scope of applications. In: Mesev, V. (Ed.) Remotely Sensed Cities. Taylor & Francis: London, UK, 281-299.
- Elvidge, C.D., Imhoff, M.L., Baugh, K.E., Hobson, V-R., Nelson, I., Safran, J., Dietz, J.B. and Tuttle, B.T., 2001a. Night-time lights of the world: 1994-1995. *ISPRS Journal of Photogrammetry & Remote Sensing*, 56, 81-99.
- Elvidge, C.D., Sutton, P.C., Baugh, K.E., Tuttle, B.T., Howard, A.T., Erwin, E.H., Bhaduri, B. and Bright E. (2006). A global poverty map derived from satellite data. Submitted to *Ambio*.
- Frank, K. D. 1998. Impact of outdoor lighting on moths: an assessment. *Journal of the Lepidopterists' Society* 42:63-93.
- Imhoff, M.L., Lawrence, W.T., Stutzer, D.C. and Elvidge, C.D. 1997. A Technique for using composite DMSP-OLS "City Lights" satellite data to map urban area. *Remote Sensing of Environment*, 61, 361-370.
- Kaufman, Y.J., Justice, C.O., Flynn L.P., Kendall, J.D., Prins, E.M., Giglio, L., Ward, D.E., Menzel, W.P. and Setzer, A.W., 1998. Potential global fire monitoring from EOS-MODIS. *Journal of Geophysical Research-Atmospheres*, 103 (D24), 32215-32238.

- Kiran Chand, T.R., Badarinath, K.V.S., Krishna Prasad, V., Murthy, M.S.R., Elvidge, Chris.D., Tuttle, Benjamin T. 2006. Monitoring forest fires over the Indian region using Defense Meteorological Satellite Program Operational Linescan System nighttime satellite data. *Remote Sensing of Environment*. (103) 165-178
- Klinkenborg, V. (2008). "Our Vanishing Night." *National Geographic*. November 2008.
- Kohiyama, M., Hayashi, H., Maki, N., Higashida, M., Kroehl, H.W., Elvidge, C.D. and Hobson, V.R. 2004. Early damaged area estimation system using DMSP-OLS night-time imagery. *International Journal of Remote Sensing*. 25 (11) 2015-2036.
- Kramer, H. J. 1994. *Observation of the Earth and its Environment - Survey of Missions and Sensors*, 2nd Edition, Springer-Verlag: Berlin & New York.
- Lohmann, K. J., B. E. Witherington, C. M. F. Lohmann, and M. Salmon. 1997. Orientation, navigation, and natal beach homing in sea turtles. Pages 107-135 in P. L. Lutz and J. A. Musick (eds.), *The biology of sea turtles*, Volume I. CRC Press, Boca Raton,
- MANTLE EPROS 2003 Presentation. Available from [http://forum.europa.eu.int/Public/irc/dsis/radstat/library?l=/epros-2004/presentations\\_previous&vm=detailed&sb=Title](http://forum.europa.eu.int/Public/irc/dsis/radstat/library?l=/epros-2004/presentations_previous&vm=detailed&sb=Title)
- Montevocchi, W. A. 2006. Influences of artificial lights on marine birds. In C. Rich and T. Longcore (eds.), *Ecological Consequences of Artificial Night Lighting*. Island Press, Washington D.C.
- NASA. 2007. *The Gateway to Astronaut photography of Earth*. Johnson Space Flight Center.
- NOAA-NGDC. (2006) Night-time lights of the World 1994-95. Stable lights data set; Available from: [http://www.ngdc.noaa.gov/dmsp/download\\_Night\\_time\\_lights\\_94-95.html](http://www.ngdc.noaa.gov/dmsp/download_Night_time_lights_94-95.html)
- NOAA-NGDC. (2006) Radiance calibrated lights 1996-97; Available from: [http://www.ngdc.noaa.gov/dmsp/download\\_rad\\_cal\\_96-97.html](http://www.ngdc.noaa.gov/dmsp/download_rad_cal_96-97.html)
- Penner, J. (ed.), Lister, D. (ed.), Griggs, D.J. (ed.), Dokken, D. and McFarland, M., 1999. *Aviation and the global atmosphere: Special report of the Intergovernmental Panel on Climate Change*. Cambridge University Press: Cambridge, UK.
- Porter, M. and Enmark, H.T., 1987, A system overview of the Airborne Visible/Infrared Imaging Spectrometer (AVIRIS). JPL Publication 87-38. Available from:
- Rich, C., and Longcore, T (Eds.). 2006. *Ecological consequences of artificial night lighting*. Island Press, Washington, D.C.
- Salmon, M. 2006. Protecting sea turtles from artificial night lighting at Florida's oceanic beaches. In C. Rich and T. Longcore (eds.), *Ecological Consequences of Artificial Night Lighting*. Island Press, Washington D.C.
- Salmon, M., B. E. Witherington, and C. D. Elvidge. 2000. Artificial lighting and the recovery of sea turtles. Pages 25-34 in N. Pilcher and G. Ismail (eds.), *Sea turtles of the Indo-Pacific: research, management and conservation*. Asean Academic Press, London.
- Saxon, E.C., Parris, T and Elvidge, C.D., 1997. *Satellite Surveillance of National CO2 Emissions from Fossil Fuels*. Development Discussion Paper No. 608. Harvard Institute for International Development, Harvard University, USA.
- Small, C., Pozzi, F. C. D. Elvidge, C.D. 2005. Spatial analysis of global urban extent from DMSP-OLS night lights. *Remote Sensing of Environment* (96) 277-291
- Stefanov, W. 2005 Personal Communication. E-mail received 9/12/05
- Stewart, J. and Warntz, W., 1958. Physics of Population Distribution. *Journal of Regional Science*, 1, 99-123.
- Sullivan, W.T. III., 1989. A 10-km resolution image of the entire night-time Earth based on cloud free satellite photographs in the 400-1100nm band. *International Journal of Remote Sensing*, 10 (1), 1-5.
- Sutton P.C., Roberts D, Elvidge C,D. and Baugh, K., 2001. Census from Heaven: An estimate of the global human population using night-time satellite imagery, *International Journal of Remote Sensing*, 22 (16), 3061-3076.
- Sutton, P. C. 2003a. A scale-adjusted measure of "urban sprawl" using nighttime satellite imagery. *Remote Sensing of Environment* 86: 353-363.
- Sutton, P., Roberts, C., Elvidge, C. and Meij, H., 1997. A comparison of nighttime satellite imagery and population density for the continental united states. *Photogrammetric Engineering and Remote Sensing*, 63 (11), 1303-1313.
- Sutton, P.C. and Costanza, R., 2002. Global estimates of market and non-market values derived from nighttime satellite imagery, landcover and ecosystem service valuation. *Ecological Economics*, 41, 509-527.
- Sutton, P.C., 2003b. Estimation of human population parameters using night-time satellite imagery. In: Mesev, V. (Ed.) *Remotely Sensed Cities*. Taylor & Francis: London, UK, 301-334.

- Tobler, W., 1969. Satellite Confirmation of Settlement Size Coefficients. *Area*, 1, 30-34.
- Toenges-Schuller, N., Stein, O., Rohrer, F., Wahner, A., Richter, A., Burrows, J.P., Beirle, S., Wagner, T., Platt, U. and Elvidge, C.D. 2006. Global distribution pattern of anthropogenic nitrogen oxide emissions: Correlation analysis of satellite measurements and model calculations. *Journal of Geophysical Research*, 111, D05312, doi:10.1029/2005JD006068.
- UN, 1995. UN Statistical Division Demographic Yearbook 1995. United Nations, (Sales No. E/F.97.XIII.1): New York, USA.
- Waluda, C.M., Yamashiro, C., Elvidge, C.D., Hobson, V.R. and Rodhouse, P.G. (2004). Quantifying light-fishing for *Dosidicus gigas* in the eastern Pacific using satellite remote sensing. *Remote Sensing of Environment*. (91) 129-133.
- Weeks, J.R. 2003 Does Night-Time Lighting Deter Crime? An Analysis of Remotely-Sensed Imagery and Crime Data,” In Victor Mesev (ed.) *Remotely-Sensed Cities*, Taylor & Francis, London.
- Welch, R. and Zupko, S., 1981. Urbanized area energy utilization patterns from DMSP data. *Photogrammetric Engineering and Remote Sensing*, 45 (2), 201-207.
- Wiese, F. K., W. A. Montevecchi, G. K. Davoren, F. Huettmann, A. W. Diamond, and J. Linke. 2001. Seabirds at risk around offshore oil platforms in the North-west Atlantic. *Marine Pollution Bulletin* 42:1285-1290.
- Wiltschko, W. and R. Wiltschko. 2002. Magnetic compass orientation in birds and its physiological basis. *Naturwissenschaften* 89:445–452.
- Wise, S. E. and B. W. Buchanan. 2005. Influence of artificial illumination on the nocturnal behavior and physiology of salamanders. In C. Rich and T. Longcore (eds.), *Ecological Consequences of Artificial Night Lighting*. Island Press, Washington D.C.
- WRI, 1996. World Resources 1996-97, A Guide to the Global Environment. A Report by The World Resources Institute, UNEP, UNDP, The World Bank. Oxford, UK: Oxford University Press.